Resource Allocation for Secure Multi-UAV Communication Systems with Multi-Eavesdropper

Ruide Li, Zhiqiang Wei, Lei Yang, Derrick Wing Kwan Ng,

Jinhong Yuan, and Jianping An

Abstract

In this paper, we study the resource allocation and trajectory design for secure unmanned aerial vehicle (UAV)-enabled communication systems, where multiple multi-purpose UAV base stations are dispatched to provide secure communications to multiple legitimate ground users (GUs) in the existence of multiple eavesdroppers (Eves). Specifically, by leveraging orthogonal frequency division multiple access (OFDMA), active UAV base stations can communicate to their desired ground users via the assigned subcarriers while idle UAV base stations can serve as jammer simultaneously for communication security provisioning. To achieve fairness in secure communication, we maximize the average minimum secrecy rate per user by jointly optimizing the communication/jamming subcarrier allocation policy and the trajectory of UAVs, while taking into account the constraints on the minimum safety distance among multiple UAVs, the maximum cruising speed, the initial/final locations, and the existence of cylindrical no-fly zones (NFZs). The design is formulated as a mixed integer non-convex optimization problem which is generally intractable. Subsequently, a computationally-efficient iterative algorithm is proposed to obtain a suboptimal solution. Simulation results illustrate that the performance of the proposed iterative algorithm can significantly improve the average minimum secrecy rate compared to various baseline schemes.

I. INTRODUCTION

The rapid growing demand on wireless communication services, e.g. ultra-high data rates and massive connectivity [2], has fueled the development of wireless networks and the mass productions of wireless devices. Despite the fruitful research in the literature for providing ubiquitous services, the performance of wireless systems is limited by the users with poor channel conditions [3], [4]. Fortunately, owing to the high flexibility and low cost in deployment of unmanned aerial vehicles (UAVs), UAV-enabled communication offers a promising

R. Li and J. An are with the School of Information and Electronics, Beijing Institute of Technology, China; Z. Wei, D. W. K. Ng, and J. Yuan are with the School of Electrical Engineering and Telecommunications, the University of New South Wales, Australia; L. Yang is with Technology and Engineering Center for Space Utilization, Chinese Academy of Sciences. (e-mail: taiyuanlaide@163.com, zhiqiang.wei@unsw.edu.au, yang.lei@csu.ac.cn, {w.k.ng, j.yuan}@unsw.edu.au, an@bit.edu.cn). This paper was presented in part at IEEE Globecom 2018 [1].

solution to tackle these challenges [5]. In particular, the high mobility of UAVs facilitates the establishment of strong line-of-sight (LoS) links to ground users (GUs). Hence, in recent years, numerous applications of UAV-enabled communication have emerged dramatically not only in the military domain, but also in the civilian and commercial domains, such as disaster relief, archeology, pollution monitoring, commodity delivery, etc. [6]. Besides, several world-leading industrial companies, such as Facebook, Google, and Qualcomm, have made advancements on their journey to deliver high-speed internet from the air by UAVs [1]. As a result, the investigation of deploying UAVs for assisting wireless networks has recently received significant attention from the academia, such as mobile relays [7], [8], aerial mobile base stations [9], [10], and UAV-enabled information dissemination and data collection [1], [11].

In practical systems, although the nature of strong LoS link grants UAV-based communication as an appealing approach to provide ubiquitous high-data rate wireless service, it also makes the communication between a UAV and ground users more susceptible to be intercepted by potential eavesdroppers (Eves) [12]. Therefore, it imposes various fundamental challenges for secure UAV communication provisioning [13]. To meet this emerging need, secure UAV communication systems with a single-UAV was studied in [8], [14]–[16] with different system settings. However, due to the stringent requirements on UAV's size, weight, and power (SWAP), the performance achieved by deploying a single-UAV is still limited [6]. To achieve a higher efficiency in secure communications, multi-UAV cooperation was adopted in [17]–[20]. In particular, a jammer UAV can fly close to a potential eavesdropper based on demand by leveraging its mobility and opportunistically transmits artificial noise signal deliberately to combat the eavesdropping channels [17]. To improve the system security performance, [18] and [19] presented a cooperative jamming approach to safeguard the UAV's communication by exploiting artificial jamming transmission from other friend UAVs in the existence of a single-eavesdropper. With the consideration of fairness in two-UAV secure communications, [20] investigated the joint power allocation and trajectory design for the maximization of the minimum secrecy rate per user when one UAV is dispatched to convey confidential messages to a ground user where another cooperative UAV transmits a jamming signal. However, in [17]–[20], the role of the UAV is fixed where a communication/jamming UAV can only provide either communication/jamming signal during the whole time horizon. In contrast, a multi-purpose UAV, which can dynamically serve as a communication UAV or a jamming UAV, provides a high flexibility in trajectory design for secure UAV communications.

For instance, when a communication UAV flies closer to an eavesdropper, it can switch its role from a communication UAV to a jamming UAV for improving the system performance of secure communication. However, an efficient algorithm for optimizing resource allocation and the trajectory of multi-purpose UAVs has not been reported, yet. Moreover, [8], [14], [17], [18] only considered the scenario of a single-user and one eavesdropper. On the other hand, although a single-user with the existence of multiple eavesdroppers in UAV-enabled communication systems was investigated in [15], [16], [19], [20], these results are not applicable to most of practical and important scenarios in the present of multiple desired users. To the best of our knowledge, secure communication problem in a more general scenario, the coexistence of multiple users and multiple eavesdroppers, is very challenging and still remained to be explored.

To unleash the potential performance of UAV-enabled communications, trajectory design or path planning has been a major research area in the existing literature. For example, [7] optimized the trajectory of a UAV to maximize the system throughput of a single-user while taking into account its maximum mobility. Authors in [21] investigated the UAV's trajectory design to guarantee secure air-to-ground communications. Although the UAV trajectory has been designed with different practical considerations [15]–[20], e.g. UAV's velocity, initial/final locations, and energy efficiency, physical geometric restriction is remained to be investigated in UAV trajectory design. For example, due to regulations for military, security, safety or privacy reasons, there are some no-fly zones (NFZs) where the flight of UAVs over those regions is prohibited [22]–[24]. Therefore, the authors of [22] proposed a control mechanism based on the geometrical tangential method of control theory to avoid a UAV flying into the NFZ. However, their proposed method only focused on the cruise constraint of the UAV due to NFZ which did not take into account any security concerns of air-to-ground data communication. Thus, with the consideration of NFZs, in our previous works [1], [25], we investigated the designs of resource allocation algorithm for UAV-enabled communication systems, where a UAV is dispatched to provide communications to multiple ground users in the present of multiple NFZs. Also, with the consideration of NFZs, the authors in [24] studied the UAV secure communication system design to serve a single-legitimate user with the presence of a malicious eavesdropper. However, the existence of NFZs complicates the design of resource allocation and the results from [1], [22]–[25] are not applicable to role switching design among UAVs.

Based on the aforementioned observations, in this paper, we consider a multi-UAV-enabled

orthogonal frequency division multiple access (OFDMA) communication systems, where multiple rotary-wing UAVs base stations are dispatched to provide communications to multiple ground users with the existence of multi-eavesdropper and NFZs. We jointly design the resource allocation, trajectory design, and role selection for secure communication. In particular, the role of each UAV can be switched dynamically between serving as a jamming UAV or information UAV in each time slot and subcarrier. The design optimization problem is non-convex and generally intractable. To handle the above challenges, we first transform the original problem into its equivalent problem, which facilitates the application of alternating optimization for obtaining a suboptimal solution. In particular, the original optimization problem is divided into three subproblems, i.e., communication resource allocation, jamming policy, and UAVs' trajectories design, which to be solved iteratively. In each iteration, the communication resource allocation is designed by solving its Lagrangian dual problem. To derive jamming policy and UAVs' trajectories, a suboptimal iterative algorithm is proposed by utilizing successive convex approximation (SCA) techniques [18]–[20] with a fast convergence.

The remainder of this paper is organized as follows. Section II introduces the system model and the problem formulation for the considered cooperative multi-UAV enabled wireless system. In Section III, we propose an efficient iterative algorithm based on the Lagrange dual problem and SCA techniques which can obtain a suboptimal solution of the design problem at hand. Section V provides numerical results to demonstrate the performance of the proposed algorithms. Finally, the paper is concluded in Section VI.

Notations: $\| \cdot \|$ denotes the vector norm. $[x]^+ = \max\{0, x\}$. $[\cdot]^{\mathrm{T}}$ denotes the transpose operation. For a vector $\mathbf{a}$, $\|\mathbf{a}\|$ represents its Euclidean norm.

II. SYSTEM MODEL

We consider a wireless communication system consisting of K_U downlink users, K_E eavesdroppers, M rotary-wing UAVs denoted by set $k_U \in \mathcal{K}_U \triangleq \{1, \cdots, K_U\}$, $k_E \in \mathcal{K}_E \triangleq \{1, \cdots, K_E\}$, and $m \in \mathcal{M} \triangleq \{1, \cdots, M\}$, respectively. In the system, we adopt the OFDMA scheme for serving multiple downlink users with different subcarriers at the same time [1], [26]. Besides, the system bandwidth is divided equally into N_{F} orthogonal subcarriers, which is denoted by set $i \in \mathcal{N}_{\mathrm{F}} \triangleq \{1, \cdots, N_{\mathrm{F}}\}$. As there are multiple eavesdroppers in the system, we exploit the geometrically distributed nature of UAVs and advocate the use of their dynamical role switching for guaranteeing secure communication. To be more specific,
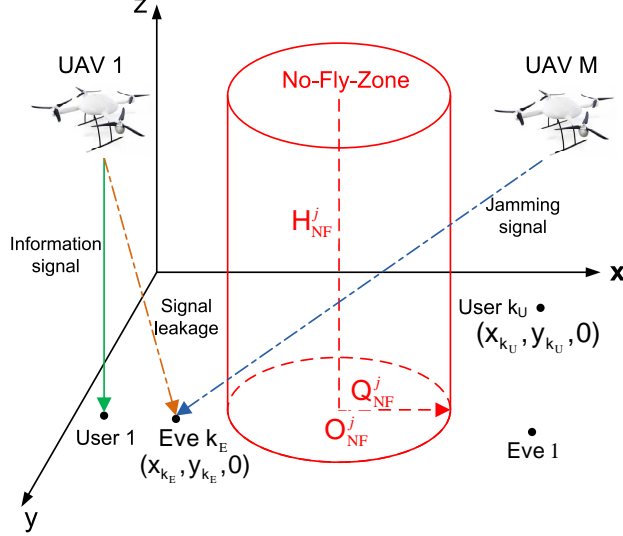
Fig. 1. Secure multi-UAV communication systems with the existence of multi-eavesdropper and a NFZ.

on each subcarrier, at a given time if a UAV[1] is selected for information transmission, the other UAVs can serve as jamming UAVs for protecting the communication via artificial noise transmission, as shown in Fig. 1. The policy adapts the communication and jamming roles of UAVs which enables a highly flexible resource allocation for improving the system performance[2].

A. Signal Model

We express the locations of all users, eavesdroppers, and UAVs in a three-dimensional (3D) Cartesian coordinate system. For the ease of design, the total time T is discretized into N time slots with equal-duration, i.e., $\delta t = T/N$, which is small enough such that the distance between the UAV and the ground user within each time slot can be treated as a constant[3]. Furthermore, we adopt n as the time slot index where $n \in \mathcal{N} \triangleq \{1, \cdots, N\}$. Thus, the ground projected trajectory of UAV m, $\mathbf{q}_m(t) = [x_m(t), y_m(t)]$, $0 \leq t \leq T$, over the time T can be approximated by a sequence $\{\mathbf{q}_m[n] = [x_m[n], y_m[n]]^T\}_{n=1}^N$, where $\mathbf{q}_m[n] \triangleq \mathbf{q}_m(n\delta t)$, $\forall n, m$, denotes the horizontal location of UAV m in time slot n. Besides, the maximum speed of each UAV are denoted as $v_{\max}$ in meters per second (m/s) and the UAV's maximum aviation distance in each time slot is $V = v_{\max}\delta t$ in meters. In particular, without lost of generality, we assume that the initial location and the final location for UAV m projected on the ground

---

[1]We assume that there are secure backhaul links for conveying a user's data between UAV and a core network which can be established by e.g. out-of-band links [9], [10].

[2]The cost of the proposed role switching is mainly on the required signaling overhead for the coordination between the cooperative UAVs.

[3]The discretized model is commonly adopted in the literature which facilitates the design of resource allocation for UAV-enabled communication systems [7], [8], [14]–[18], [20].

is $\mathbf{q}_m[0] = [x_m[0], y_m[0]]^T$ and $\mathbf{q}_m[N] = [x_m[N], y_m[N]]^T$, and the horizontal coordinates for user k_U and Eve k_E are denoted by $\mathbf{w}_{k_U} = [x_{k_U}, y_{k_U}]^T$ and $\mathbf{w}_{k_E} = [x_{k_E}, y_{k_E}]^T$, respectively. Then, the distance between UAV m and user k_U in time slot n can be written as

$$d_{m,k_U}[n] = \sqrt{||\mathbf{q}_m[n] - \mathbf{w}_{k_U}||^2 + H^2}, \ \forall n, m, k_U, \qquad (1)$$

where H in meters is the constant flying altitude of each UAV for satisfying some safety regulations. Similarly, the distance between UAV m and Eve k_E in time slot n is given by

$$d_{m,k_E}[n] = \sqrt{||\mathbf{q}_m[n] - \mathbf{w}_{k_E}||^2 + H^2}, \ \forall n, m, k_E. \qquad (2)$$

B. No-Fly-Zone Model

In practice, UAVs flying over some specific regions, known as NFZ, such as airports, prisons, military locations, and etc. are prohibited. Hence, a practical UAV-based communication system should design the UAV trajectory with the consideration of NFZs. In this paper, we assume that there are N_{NF} non-overlapped NFZs. Specifically, to guarantee the effectiveness of our UAV trajectory design, we define NFZ $j \in \{1, ..., N_{\mathrm{NF}}\}$, as a cylindrical volume with a center coordinate $\mathbf{w}_{\mathrm{NF}}^j = [x_{\mathrm{NF}}^j, y_{\mathrm{NF}}^j]^T$ projected on the ground, height H_{NF}^j, $H < H_{\mathrm{NF}}^j$, $\forall j$, and radius Q_{NF}^j, $\forall j$, cf. Fig. 1. With the existence of NFZs, the trajectory of UAV m should satisfy the following inequality in each time slot:

$$||\mathbf{q}_m[n] - \mathbf{w}_{\mathrm{NF}}^j||^2 \geq \left(Q_{\mathrm{NF}}^j\right)^2, \ \forall n, m, j. \qquad (3)$$

Remark 1: A reasonable UAV trajectory should be planed such that a UAV can follow the desired path as tightly as possible. Based on the geometric and kinematics properties, cylindrical volumn models for NFZ satisfy lateral guidance control law of UAVs which are commonly adopted for the design of flight path, e.g. [27], [28]. When a UAV has to avoid flying over NFZs, a centripetal acceleration on the UAV is generated to help the UAV change its aviation direction. The centripetal acceleration is related to the UAV's radial flying velocity and radius of turning circle, which leads to a circular trajectory when the UAV turns steadily [29]. Therefore, for the purpose to design a more practical NFZ model so that a UAV can tightly follow its desired flight path, NFZs are modeled by cylindrical volume constraints in this paper.

C. Channel Model

We assume that the wireless channels from a UAV to the ground user/Eve on each subcarrier are LoS-dominated and we adopt the commonly used free-space path loss model[4] as in [6]-

---

[4]We note that field measurements [30] suggest that air-to-ground links are almost guaranteed to be LoS channels in rural areas when a UAV flies with an altitude of 100 meters or above to serve a cell with a radius of 500 meters. Furthermore, the aviation altitude of a UAV can be adjusted according to the type of terrain and the scale of the cells, which can guarantee that the air-to-ground channel LoS probability approaches one [31].

[7]. Furthermore, we assume that the Doppler effect caused by the mobility of UAVs can be well compensated by all the receivers[5]. Thus, the channel power gain from UAV m to ground user k_U in time slot n can be given by

$$h_{m,k_U}[n] = \beta_0 d_{m,k_U}^{-2}[n] = \frac{\beta_0}{||\mathbf{q}_m[n] - \mathbf{w}_{k_U}||^2 + H^2}, \ \forall n, m, k_U, \tag{4}$$

where β_0 denotes the channel power gain at the reference distance $d_0 = 1$ m. Similarly, channel power gains from UAV m to Eve k_E in time slot n can be written as

$$h_{m,k_E}[n] = \beta_0 d_{m,k_E}^{-2}[n] = \frac{\beta_0}{||\mathbf{q}_m[n] - \mathbf{w}_{k_E}||^2 + H^2}, \ \forall n, m, k_E. \tag{5}$$

D. Communication & Jamming Scheduling Model

To prevent multiple access interference from all the communication UAVs, in time slot n, we assume that there is at most one UAV communicates with at most one user on subcarrier i. On the other hand, since there are multiple Eves randomly distributed on the ground and multiple UAVs in the sky, when subcarrier i is not assigned to UAV m for information transmission, UAV m can act as a jammer on this subcarrier to combat the channel of Eves. For the sake of presentation and to facilitate the solution design, we denote $s_{m,k_U,i}[n] \in \{0, 1\}$ and $s_{m,i}^J[n] \in \{0, 1\}$ as binary variables, which indicates that if UAV m communicates with user k_U, i.e., $s_{m,k_U,i}[n] = 1$ or acts as a jammer, i.e., $s_{m,i}^J[n] = 1$ in time slot n on subcarrier i, respectively. In particular, the binary variables satisfy the following constraints:

$$s_{m,k_U,i}[n] \in \{0, 1\}, \forall n, m, k_U, i, \tag{6}$$

$$s_{m,i}^J[n] \in \{0, 1\}, \forall n, m, i, \tag{7}$$

$$\sum_{m=1}^{M} \sum_{k_U=1}^{K_U} s_{m,k_U,i}[n] \leq 1, \qquad \forall n, i, \tag{8}$$

$$\sum_{k_U=1}^{K_U} s_{m,k_U,i}[n] + s_{m,i}^J[n] \leq 1, \qquad \forall n, m, i. \tag{9}$$

III. Problem Formulation

In this section, we first define the achievable rate and secrecy rate for the considered multi-UAV system. Then, the multi-UAV secure communication system design is formulated as a non-convex optimization problem.

---

[5]This assumption is commonly used in the research of UAV communications [18], [32]–[35], since the impact of frequency offset caused by the high mobility of UAV has been well studied in the literature which can be well compensated by using some Doppler effect compensation technologies [36]–[38].

A. Achievable Rate & Secrecy Rate

Denote $p_{m,k_U,i}[n] \geq 0$ as the communication power from UAV m to user k_U in time slot n on subcarrier i, $p_{m,i}^J[n] \geq 0$ as the jamming power from UAV m in time slot n on subcarrier i, and P_{peak}^m the peak transmission power of UAV m. Then, we have

$$0 \leq \underbrace{\sum_{k_U=1}^{K_U} \sum_{i=1}^{N_F} s_{m,k_U,i}[n]p_{m,k_U,i}[n]}_{\text{Information power}} + \underbrace{\sum_{i=1}^{N_F} s_{m,i}^J[n]p_{m,i}^J[n]}_{\text{Jamming power}} \leq P_{\text{peak}}^m, \ \forall n, m. \tag{10}$$

Thus, if UAV m is selected to communicate to user k_U in time slot n on subcarrier i, i.e., $s_{m,k_U,i}[n] = 1$, the received signal-to-interference-plus-noise ratio (SINR) at user k_U on subcarrier i in time slot n can be written as

$$\gamma_{m,k_U,i}[n] = \frac{p_{m,k_U,i}[n]h_{m,k_U}[n]}{I_{m,k_U,i}[n] + \sigma^2}, \ \forall n, m, k_U, i, \tag{11}$$

where σ^2 denotes the additive white Gaussian noise (AWGN) power at ground users and

$$I_{m,k_U,i}[n] = \sum_{m'=1,m' \neq m}^{M} s_{m',i}^J[n]p_{m',i}^J[n]h_{m',k_U}[n], \forall n, m, k_U, i, \tag{12}$$

represents the co-channel interference caused by UAV $m' \in \mathcal{M}, m' \neq m$, to user k_U on subcarrier i.

On the other hand, the received SINR at Eve k_E from UAV m for attempting to decode the signal of user k_U in time slot n on subcarrier i can be written as

$$\gamma'_{m,k_U,k_E,i}[n] = \frac{p_{m,k_U,i}[n]h_{m,k_E}[n]}{I_{m,k_E,i}[n] + \sigma^2}, \ \forall n, m, k_U, k_E, i, \tag{13}$$

where

$$I_{m,k_E,i}[n] = \sum_{m'=1,m' \neq m}^{M} s_{m',i}^J[n]p_{m',i}^J[n]h_{m',k_E}[n], \forall n, m, k_E, i, \tag{14}$$

is the interference to Eve k_E on subcarrier i in time slot n.

Thus, the communication rate $R_{m,k_U,i}[n]$ from UAV m to user k_U in time slot n on subcarrier i in bits/second/Hertz (bps/Hz) is given by

$$R_{m,k_U,i}[n] = s_{m,k_U,i}[n] \log_2\left(1 + \gamma_{m,k_U,i}[n]\right), \ \forall n, m, k_U, i, \tag{15}$$

while the corresponding leakage rate $R'_{m,k_E,i}[n]$ to Eve k_E can be written as

$$R'_{m,k_U,k_E,i}[n] = s_{m,k_U,i}[n] \log_2\left(1 + \gamma'_{m,k_U,k_E,i}[n]\right), \ \forall n, m, k_U, k_E, i. \tag{16}$$

Then, the average secrecy rate $\bar{R}_{k_U}^s$ in bps/Hz over N time slots for user k_U considered with K_E eavesdroppers is given by

$$\bar{R}_{k_U}^s = \frac{1}{N} \sum_{n=1}^{N} \sum_{m=1}^{M} \sum_{i=1}^{N_F} \left[R_{m,k_U,i}[n] - \max_{k_E \in \mathcal{K}_E} \left\{ R'_{m,k_U,k_E,i}[n] \right\} \right]^+, \forall k_U. \tag{17}$$

B. Optimization Problem Formulation

For notational simplicity, we denote $\mathcal{Q} = \{\mathbf{q}_m[n], \forall n, m\}$ as the set of all UAVs' trajectory variables, $\mathcal{S}_U = \{s_{m,k_U,i}[n], \forall n, m, k_U, i\}$ as the set of the communication scheduling variables, $\mathcal{S}_J = \{s^J_{m,i}[n], \forall n, m, i\}$ as the set of the jamming scheduling variables. Let $\mathcal{P}_U = \{p_{m,k_U,i}[n], \forall n, m, k_U, i\}$ denote the set of all the communication UAVs' transmit power variables and $\mathcal{P}_J = \{p^J_{m,i}[n], \forall n, m, i\}$ denote the set of the jamming power variables from all jamming UAVs.

We aim to maximize the average minimum secrecy rate among all ground users via jointly optimizing communication scheduling, communication power, jamming scheduling, jamming power, and all UAVs' trajectories. Define η as an auxiliary optimization variable and the max-min fairness optimization problem can be formulated as

$$\underset{\eta, \mathcal{Q}, \mathcal{S}_U, \mathcal{S}_J, \mathcal{P}_U, \mathcal{P}_J}{\text{maximize}} \quad \eta \tag{18}$$

$$\text{s.t.} \ \text{C1}: \frac{1}{N} \sum_{n=1}^{N} \sum_{m=1}^{M} \sum_{i=1}^{N_{\text{F}}} \left[R_{m,k_U,i}[n] - R'_{m,k_U,k_E,i}[n] \right]^+ \geq \eta, \forall k_U, k_E,$$

$$\text{C2}: s_{m,k_U,i}[n] \in \{0,1\}, \forall n, m, k_U, i,$$

$$\text{C3}: s^J_{m,i}[n] \in \{0,1\}, \forall n, m, i,$$

$$\text{C4}: \sum_{m=1}^{M} \sum_{k_U=1}^{K_{\text{U}}} s_{m,k_U,i}[n] \leq 1, \forall n, i,$$

$$\text{C5}: \sum_{k_U=1}^{K_{\text{U}}} s_{m,k_U,i}[n] + s^J_{m,i}[n] \leq 1, \forall n, m, i,$$

$$\text{C6a}: \sum_{k_U=1}^{K_{\text{U}}} \sum_{i=1}^{N_{\text{F}}} s_{m,k_U,i}[n] p_{m,k_U,i}[n] + \sum_{i=1}^{N_{\text{F}}} s^J_{m,i}[n] p^J_{m,i}[n] \leq P^m_{\text{peak}}, \ \forall n, m,$$

$$\text{C6b}: p_{m,k_U,i}[n] \geq 0, \forall n, m, k_U, i, \qquad \text{C6c}: p^J_{m,i}[n] \geq 0, \forall n, m, i,$$

$$\text{C7}: ||\mathbf{q}_m[n] - \mathbf{q}_m[n-1]||^2 \leq V^2, \forall n, m,$$

$$\text{C8}: ||\mathbf{q}_m[n] - \mathbf{w}^j_{\text{NF}}||^2 \geq \left(Q^j_{\text{NF}}\right)^2, \forall n, m, j,$$

$$\text{C9}: ||\mathbf{q}_m[n] - \mathbf{q}_{m'}[n]||^2 \geq D^2_{\text{S}}, \forall n, m, m \neq m',$$

$$\text{C10}: \mathbf{q}_m[0] = \mathbf{q}^0_m, \forall m, \qquad\qquad \text{C11}: \mathbf{q}_m[N] = \mathbf{q}^F_m, \forall m,$$

where constraint C1 is imposed to guarantee an average minimum secrecy rate η for each user over all time slots. C2 and C3 are the binary constraints to denote the UAV's communication and jamming subcarrier allocation, respectively. Constraint C4 is imposed to make sure that in any time slot, each subcarrier can be allocated to at most one user for communication from
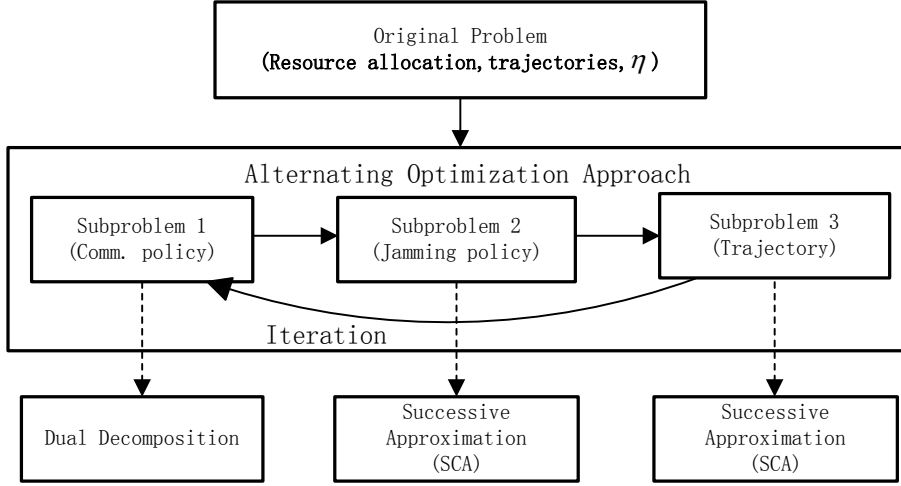
Fig. 2. A flow chart of the proposed iterative algorithm.

all the UAVs. Constraint C5 is introduced such that a UAV can either transmit information or jamming signal on each subcarrier. Constraints C6a−C6c are the UAV transmission power constraints, P_{peak}^m in C6a denotes the maximum transmission power of UAV m, C6b and C6c are the non-negative constraints on the power allocation variables. Constraint C7 is imposed to ensure that each UAV should fly no faster than its maximum speed V in each time slot. Constraint C8 states that a UAV is prohibited to fly over the NFZs. D_{S} in constraint C9 is the minimum distance between any UAV pairs to avoid collision. Constraints C10 and C11 indicate the fixed initial and final locations of the UAVs, $\mathbf{q}_m^0 = [x_m[0], y_m[0]]^T$ and $\mathbf{q}_m^F = [x_m[N], y_m[N]]^T$, respectively.

IV. JOINT TRAJECTORY AND RESOURCE ALLOCATION DESIGN

The formulated problem in (18) is a mixed-integer non-convex and generally intractable. Specifically, the main obstacle in solving (18) arises from the binary constraints C2 and C3 while the non-convexity originates from C1, C6a, C8, and C9. Besides, the problem is further complicated by the coupling between binary and continuous variables in C1 and C6a. Therefore, obtaining the globally optimal solution requires a prohibitively large computational complexity which is not practical even for moderate system size. As a compromise approach, in this section, we propose a series of transformation which facilitates the development of a

low-complexity algorithm for achieving a suboptimal solution[6]. To this end, we first propose Lemma 1 to handle the non-smoothness function due to the $[\cdot]^+$ operation in constraint C1 of problem (18).

Lemma 1: Problem (18) has the same optimal solution as the following problem:

$$\underset{\eta,\mathcal{Q},\mathcal{S}_U,\mathcal{S}_J,\mathcal{P}_U,\mathcal{P}_J}{\text{maximize}} \eta \tag{19}$$

$$\text{s.t.} \quad \text{C2}-\text{C11},$$

$$\text{C1}: \frac{1}{N} \sum_{n=1}^{N} \sum_{m=1}^{M} \sum_{i=1}^{N_{\mathrm{F}}} R_{m,k_U,i}[n] - R'_{m,k_U,k_E,i}[n] \geq \eta, \forall k_U, k_E.$$

Proof 1: Please refer to Appendix A for a proof of Lemma 1.

Although problem (19) is easier to handle, it is still non-convex and challenging to solve. Next, we divide problem (19) into three subproblems with three individual sets of optimization variables, respectively, i.e., $(\eta, \mathcal{S}_U, \mathcal{P}_U)$, $(\eta, \mathcal{S}_J, \mathcal{P}_J)$, $(\eta, \mathcal{Q})$, which facilitates the design of a computationally efficient iterative alternating algorithm to achieve a suboptimal solution, cf. Fig. 2. In particular, we first jointly optimize the average minimum secrecy data rate, communication user scheduling, and communication power of each UAV. Then, with fixed trajectories and obtained communication policy, we study the jamming scheduling and jamming power allocation, for obtaining an intermediate optimized average minimum secrecy data rate. In the last subproblem, we design all UAVs' trajectories and update the average minimum secrecy data rate with the above obtained resource allocation policy.

A. Subproblem 1: Communication Resource Allocation Optimization

In this section, we consider subproblem 1 for optimizing the communication user scheduling and communication power by assuming that jamming policy $(\mathcal{S}_J, \mathcal{P}_J)$ and all UAVs'

---

[6]In fact, the designed suboptimal algorithm requires only a polynomial time computational complexity which is suitable for realtime implementations [39]. In the considered system, the algorithm can be executed by the UAV-onboard computing system or with the help of a ground station via computation offloading [40].

trajectories $\mathcal{Q}$ are fixed. Thus, subproblem 1 can be written as:

$$\underset{\eta,\mathcal{S}_U,\mathcal{P}_U}{\text{maximize}} \ \eta \tag{20}$$

$$\text{s.t.} \ \text{C1}: \frac{1}{N}\sum_{n=1}^{N}\sum_{m=1}^{M}\sum_{i=1}^{N_F} R_{m,k_U,i}[n] - R'_{m,k_U,k_E,i}[n] \geq \eta, \forall k_U, k_E,$$

$$\text{C2}: s_{m,k_U,i}[n] \in \{0,1\}, \forall n, m, k_U, i, \quad \text{C4}: \sum_{m=1}^{M}\sum_{k_U=1}^{K_U} s_{m,k_U,i}[n] \leq 1, \forall n, i,$$

$$\text{C5}: \sum_{k_U=1}^{K_U} s_{m,k_U,i}[n] + s_{m,i}^J[n] \leq 1, \forall n, m, i,$$

$$\text{C6a}: \sum_{k_U=1}^{K_U}\sum_{i=1}^{N_F} s_{m,k_U,i}[n]p_{m,k_U,i}[n] + \sum_{i=1}^{N_F} s_{m,i}^J[n]p_{m,i}^J[n] \leq P_{\text{peak}}^m, \ \forall n, m,$$

$$\text{C6b}: p_{m,k_U,i}[n] \geq 0, \forall n, m, k_U, i.$$

In order to solve subproblem 1 in (20), by following a similar approach as [16], [41], we introduce an auxiliary variable $\widetilde{p}_{m,k_U,i}[n] = s_{m,k_U,i}[n]p_{m,k_U,i}[n]$, and the problem can be equivalently written as

$$\underset{\eta,\mathcal{S}_U,\widetilde{\mathcal{P}}_U}{\text{maximize}} \ \eta \tag{21}$$

$$\text{s.t.} \ \widetilde{\text{C1}}: \frac{1}{N}\sum_{n=1}^{N}\sum_{m=1}^{M}\sum_{i=1}^{N_F} \widetilde{R}_{m,k_U,i}[n] - \widetilde{R}'_{m,k_U,k_E,i}[n] \geq \eta, \forall k_U, k_E,$$

$$\text{C2}: s_{m,k_U,i}[n] \in \{0,1\}, \forall n, m, k_U, i, \quad \text{C4}: \sum_{m=1}^{M}\sum_{k_U=1}^{K_U} s_{m,k_U,i}[n] \leq 1, \forall n, i,$$

$$\text{C5}: \sum_{k_U=1}^{K_U} s_{m,k_U,i}[n] + s_{m,i}^J[n] \leq 1, \forall n, m, i,$$

$$\widetilde{\text{C6a}}: \sum_{k_U=1}^{K_U}\sum_{i=1}^{N_F} \widetilde{p}_{m,k_U,i}[n] + \sum_{i=1}^{N_F} s_{m,i}^J[n]p_{m,i}^J[n] \leq P_{\text{peak}}^m, \ \forall n, m,$$

$$\widetilde{\text{C6b}}: \widetilde{p}_{m,k_U,i}[n] \geq 0, \forall n, m, k_U, i,$$

where $\widetilde{\mathcal{P}}_U = \{\widetilde{p}_{m,k_U,i}[n], \forall n, m, i, k_U\}$,

$$\widetilde{R}_{m,k_U,i}[n] = s_{m,k_U,i}[n]\log_2\left(1 + \frac{\widetilde{p}_{m,k_U,i}[n]\mathcal{H}_{m,k_U,i}[n]}{s_{m,k_U,i}[n]}\right), \forall n, m, k_U, i, \tag{22}$$

$$\widetilde{R}'_{m,k_U,k_E,i}[n] = s_{m,k_U,i}[n]\log_2\left(1 + \frac{\widetilde{p}_{m,k_U,i}[n]\mathcal{H}'_{m,k_E,i}[n]}{s_{m,k_U,i}[n]}\right), \forall n, m, k_U, k_E, i, \tag{23}$$

$$\mathcal{H}_{m,k_U,i}[n] = \frac{h_{m,k_U}[n]}{I_{m,k_U,i}[n] + \sigma^2}, \forall n, m, k_U, i, \tag{24}$$

$$\mathcal{H}'_{m,k_E,i}[n] = \frac{h_{m,k_E}[n]}{I_{m,k_E,i}[n] + \sigma^2}, \forall n, m, k_E, i. \tag{25}$$

Next, we handle the binary user scheduling constraint C2 in (21). In particular, we follow a similar approach as in [1], [41] and relax the binary subcarrier variable $s_{m,k_U,i}[n]$ as a real value between 0 and 1, i.e.,

$$\widetilde{\text{C2}} : 0 \leq s_{m,k_U,i}[n] \leq 1, \forall n, m, k_U, i. \tag{26}$$

Meanwhile, the relaxed variable $s_{m,k_U,i}[n]$ serves as a time-sharing factor for user k_U on subcarrier i in time slot n.

After replacing C2 with $\widetilde{\text{C2}}$ in (21), the problem can be written[7] as

$$\underset{\eta, \mathcal{S}_U, \tilde{\mathcal{P}}_U}{\text{maximize}} \ \eta \tag{27}$$

$$\text{s.t.} \quad \widetilde{\text{C1}}, \text{C4} - \widetilde{\text{C6b}},$$

$$\widetilde{\text{C2}} : \ 0 \leq s_{m,k_U,i}[n] \leq 1, \forall n, m, k_U, i.$$

Then, before we derive the optimal communication resource allocation, we first verify the convexity of constraint $\widetilde{\text{C1}}$ jointly with respect to (w.r.t.) $\tilde{s}_{m,k_U,i}[n]$ and $\tilde{p}_{m,k_U,i}[n]$ via the following lemma:

Lemma 2: For $\kappa_1 > \kappa_2 \geq 0$, the function $\psi(x,y) \triangleq x\log_2(1 + \frac{\kappa_1 y}{x}) - x\log_2(1 + \frac{\kappa_2 y}{x})$ is concave w.r.t. $x \geq 0$ and $y \geq 0$.

Proof 2: Please refer to Appendix B for a proof of Lemma 2.

In other words, with $\mathcal{H}_{m,k_U,i}[n] > \mathcal{H}'_{m,k_E,i}[n]$, constraint $\widetilde{\text{C1}}$ is jointly concave w.r.t. $\mathcal{S}_U$ and $\tilde{\mathcal{P}}_U$ which satisfies Lemma 2. Next, we consider the communication resource allocation under $\mathcal{H}_{m,k_U,i}[n] > \mathcal{H}'_{m,k_E,i}[n]$, and study the convexity of constraint $\widetilde{\text{C1}}$ under such a condition.

Lemma 3: For the problem in (21), if $\mathcal{H}_{m,k_U,i}[n] \leq \mathcal{H}'_{m,k_E,i}[n]$, UAV m would not allocate any power for user k_U on subcarrier i in time slot n, i.e., $s_{m,k_U,i}[n] = 0$ and $\tilde{p}_{m,k_U,i}[n] = 0$.

Proof 3: Please refer to Appendix C for a proof of Lemma 3.

Now, problem (27) is jointly convex w.r.t. $\eta, \tilde{s}_{m,k_U,i}[n]$, and $\tilde{p}_{m,k_U,i}[n]$. Furthermore, problem (27) satisfies the Slater's constraint qualification and thus the strong duality holds [42]–[44]. Therefore, the duality gap is zero. In other words, the optimal solution of problem (27) can be obtained by solving its dual problem. To shed lights on important system design

---

[7]We note that the adopted constraint relaxation is tight as will be shown in the following.

insights, we solve the dual problem via deriving some semi-closed-form solutions. To this end, we first derive the Lagrangian of problem (27):

$$\mathcal{L}(\eta, \boldsymbol{\alpha}, \boldsymbol{\beta}, \boldsymbol{\varepsilon}, \boldsymbol{\vartheta}, \mathcal{S}_U, \tilde{\mathcal{P}}_U) \tag{28}$$

$$= \eta - \sum_{k_U=1}^{K_U} \sum_{k_E=1}^{K_E} \alpha_{k_U, k_E} \left(N\eta - \sum_{n=1}^{N} \sum_{m=1}^{M} \sum_{i=1}^{N_F} [\tilde{R}_{m,k_U,i}[n] - \widetilde{R}'_{m,k_U,k_E,i}[n]] \right) - \sum_{n=1}^{N} \sum_{i=1}^{N_F} \beta_i[n] \left(\sum_{m=1}^{M} \sum_{k_U=1}^{K_U} s_{m,k_U,i}[n] - 1 \right)$$

$$- \sum_{n=1}^{N} \sum_{m=1}^{M} \left[\sum_{i=1}^{N_F} \varepsilon_{m,i}[n] \left(\sum_{k_U=1}^{K_U} s_{m,k_U,i}[n] + s_{m,i}^J[n] - 1 \right) - \vartheta_m[n] \left(\sum_{k_U=1}^{K_U} \sum_{i=1}^{N_F} \tilde{p}_{m,k_U,i}[n] + \sum_{i=1}^{N_F} s_{m,i}^J p_{m,i}^J[n] - P_{\text{peak}}^m \right) \right],$$

where $\boldsymbol{\alpha} = \{\alpha_{k_U, k_E} \geq 0, \forall k_U, k_E\}$, $\boldsymbol{\beta} = \{\beta_i[n] \geq 0, \forall n, i\}$, $\boldsymbol{\varepsilon} = \{\varepsilon_{m,i}[n] \geq 0, \forall n, m, i\}$, and $\boldsymbol{\vartheta} = \{\vartheta_m[n] > 0, \forall n, m\}$, denote the Lagrange multipliers for constraints $\widetilde{\text{C1}}$, C4, C5, and $\widetilde{\text{C6a}}$, respectively. Constraints C2 and $\widetilde{\text{C6b}}$ will be considered when deriving the optimal solution via examining the Karush-Kuhn-Tucker (KKT) conditions in the following. Thus, the dual problem of (27) can be written as

$$\mathcal{D} = \underset{\boldsymbol{\alpha}, \boldsymbol{\beta}, \boldsymbol{\varepsilon}, \boldsymbol{\vartheta} \geq 0}{\text{minimize}} \ \underset{\eta, \mathcal{S}_U, \tilde{\mathcal{P}}_U}{\text{maximize}} \ \mathcal{L}(\eta, \boldsymbol{\alpha}, \boldsymbol{\beta}, \boldsymbol{\varepsilon}, \boldsymbol{\vartheta}, \mathcal{S}_U, \tilde{\mathcal{P}}_U). \tag{29}$$

Then, by using dual decomposition [45], the dual problem can be solved iteratively by solving the two layers which is divided from the dual problem: Layer 1, maximizing the Lagrangian over minimum secrecy rate η, user scheduling $\mathcal{S}_U$, and power allocation $\tilde{\mathcal{P}}_U$ in (29), for given Lagrange multipliers $\boldsymbol{\alpha}, \boldsymbol{\beta}, \boldsymbol{\varepsilon}$, and $\boldsymbol{\vartheta}$; Layer 2, minimizing the Lagrangian function over $\boldsymbol{\alpha}, \boldsymbol{\beta}, \boldsymbol{\varepsilon}$, and $\boldsymbol{\vartheta}$ in (29), for a fixed minimum secrecy rate η, user scheduling $\mathcal{S}_U$, and power allocation $\tilde{\mathcal{P}}_U$.

Solution of Layer 1 (Power Allocation and User Scheduling): Denote $s_{m,k_U,i}^*[n]$, $p_{m,k_U,i}^*[n]$, and $\widetilde{p}_{m,k_U,i}^*[n]$ the optimal solutions of subproblem 1. Thus, the optimal power allocation for user k_U on subcarrier i in time slot n is given by

$$\widetilde{p}_{m,k_U,i}^*[n] = s_{m,k_U,i}[n] p_{m,k_U,i}^*[n] \tag{30}$$

$$= \frac{s_{m,k_U,i}[n]}{2} \left[\sqrt{\Gamma_{m,k_U,k_E,i}^2[n] + \frac{4\alpha_{k_U,k_E}}{\vartheta_m[n] \ln 2} \Gamma_{m,k_U,k_E,i}[n]} - \left(\frac{1}{\mathcal{H}'_{m,k_E,i}[n]} + \frac{1}{\mathcal{H}_{m,k_U,i}[n]} \right) \right]^+,$$

where $\Gamma_{m,k_U,k_E,i}[n] = \left(\frac{1}{\mathcal{H}'_{m,k_E,i}[n]} - \frac{1}{\mathcal{H}_{m,k_U,i}[n]} \right)$.

We note that the solution derived in (30) coincides Lemma 3 where no power is allocated on subcarrier i from UAV m if $\mathcal{H}_{m,k_U,i}[n] \leq \mathcal{H}'_{m,k_E,i}[n]$. Lagrange multipliers α_{k_U,k_E} and $\vartheta_m[n]$ in (30) ensure that the average minimum secrecy rate constraint $\widetilde{\text{C1}}$ and the maximum transmission power constraint $\widetilde{\text{C6a}}$ are satisfied, respectively, when the optimal solution of (27) is attained. In general, the water-level for user k_U, i.e. $\frac{4\alpha_{k_U,k_E}}{\vartheta_m[n] \ln 2} \Gamma_{m,k_U,k_E,i}[n]$, is different

from other users on subcarrier i in time slot n. According to the KKT conditions [42], the following equality holds at the optimal point of the problem in (21):

$$\alpha_{k_U,k_E}\left(\sum_{n=1}^{N}\sum_{m=1}^{M}\sum_{i=1}^{N_F}\left[R_{m,k_U,i}[n]-\widetilde{R}'_{m,k_U,k_E,i}[n]\right]-N\eta\right)=0, \forall k_U, k_E. \tag{31}$$

Therefore, Lagrange multiplier α_{k_U,k_E} is used to adjust the resource allocation such that constraint C1 is satisfied with equality. In fact, it reallocates the resource from the stronger users to weaker users to achieve certain fairness between users. On the other hand, Lagrange multiplier $\vartheta_m[n] > 0$ adjusts the water level to satisfy constraint $\widetilde{C6a}$. Then, the optimal subcarrier allocation can be obtained via the derivative of the Lagrangian function w.r.t. $s_{m,k_U,i}[n]$, which yields

$$S_{m,k_U,i}[n]=\alpha_{k_U,k_E}\left(\log_2\left(\frac{1+\Lambda_{m,k_U,i}[n]}{1+\Lambda'_{m,k_U,k_E,i}[n]}\right)-\frac{\Lambda_{m,k_U,i}[n]}{(1+\Lambda_{m,k_U,i}[n])\ln 2}+\frac{\Lambda'_{m,k_U,k_E,i}[n]}{\left(1+\Lambda'_{m,k_U,k_E,i}[n]\right)\ln 2}\right)-\beta_i[n]-\varepsilon_{m,i}[n],$$
$$\tag{32}$$

where $\Lambda_{m,k_U,i}[n] = p_{m,k_U,i}[n]\mathcal{H}_{m,k_U,i}[n]$ and $\Lambda'_{m,k_U,k_E,i}[n] = p_{m,k_U,i}[n]\mathcal{H}'_{m,k_E,i}[n]$. Since (32) is independent of $s_{m,k_U,i}[n]$, with the consideration of constraint C4, the optimal user scheduling on subcarrier i for UAV m in each time slot n is given by

$$s^*_{m,k_U,i}[n] = \begin{cases} 1, & m^*, k_U^* = \max_{m,k_U}(S_{m,k_U,i}[n]), \\ 0, & \text{otherwise,} \end{cases} \quad \forall n,i, \tag{33}$$

the solution is still binary, which means that the relaxation adopted in $\widetilde{C2}$ is tight.

Solution of Layer 2 (Master Problem): To solve the master minimization problem in (29), we adopt the gradient method to update the Lagrange multipliers which is given by

$$\alpha_{k_U,k_E}(l_1+1)=\left[\alpha_{k_U,k_E}(l_1)-\delta_1(l_1)\times\left(\frac{1}{N}\sum_{n=1}^{N}\sum_{m=1}^{M}\sum_{i=1}^{N_F}\left[R_{m,k_U,i}[n]-R'_{m,k_U,k_E,i}[n]\right]-\eta\right)\right]^+, \forall k_U, k_E, \tag{34}$$

$$\beta_i[n](l_1+1)=\left[\beta_i[n](l_1)-\delta_2(l_1)\times\left(1-\sum_{m=1}^{M}\sum_{k_U=1}^{K_U}s_{m,k_U,i}[n]\right)\right]^+, \forall n,i, \tag{35}$$

$$\varepsilon_{m,i}[n](l_1+1)=\left[\varepsilon_{m,i}[n](l_1)-\delta_3(l_1)\times\left(1-\sum_{k_U=1}^{K_U}s_{m,k_U,i}[n]-s^J_{m,i}[n]\right)\right]^+, \forall n,m,i, \tag{36}$$

$$\vartheta_m[n](l_1+1)=\left[\vartheta_m[n](l_1)-\delta_4(l_1)\times\left(P^m_{\text{peak}}-\sum_{k_U=1}^{K_U}\sum_{i=1}^{N_F}\widetilde{p}_{m,k_U,i}[n]-\sum_{i=1}^{N_F}s^J_{m,i}[n]p^J_{m,i}[n]\right)\right]^+, \forall n,m, \tag{37}$$

where $l_1 \geq 0$ is the iteration index for subproblem 1 and $\delta_u(l_1), u \in \{1,\dots,4\}$, is the step size [41]. Thus, subproblem Layer 1 in problem (29) can be solved by using the updated Lagrangian multipliers in (34)-(37). The proposed Algorithm for solving subproblem 1 is summarized in **Algorithm 1**. Specifically, we solve the power allocation and user scheduling via the semi-closed-form solutions in (30) and (33), respectively, with a given Lagrange

---

Algorithm 1 Optimal User Scheduling and Power Allocation for Subproblem 1

1: Initialize the maximum number of iterations $L_{\text{max\_inner}}^{l_1}$, $L_{\text{max\_outer}}^{l_1}$, and the maximum tolerance $\epsilon_{\text{inner}}^{l_1}$, $\epsilon_{\text{outer}}^{l_1}$ for inner
   loop and outer loop, respectively.

2: Set intermediate average minimum secrecy rate $\eta^{(0)} = 0$, iteration index $l_1^{\text{inner}} = 0$, and $l_1 = 0$ for inner loop and
   outer loop, respectively.

3: **repeat** {Power Allocation and User Scheduling}

4:    Maximize the Lagrangian over the minimum secrecy rate η, user scheduling $\mathcal{S}_U$, and power allocation $\tilde{\mathcal{P}}_U$ in (29)
      with the given Lagrange multipliers $\boldsymbol{\alpha}, \boldsymbol{\beta}, \boldsymbol{\varepsilon}, \boldsymbol{\vartheta}$.

5:    **repeat** {Master Problem}

6:       Minimize the Lagrangian function in (29) over the Lagrange multipliers $\boldsymbol{\alpha}, \boldsymbol{\beta}, \boldsymbol{\varepsilon}, \boldsymbol{\vartheta}$, for a fixed minimum secrecy
         rate η, user scheduling $\mathcal{S}_U$, and power allocation $\tilde{\mathcal{P}}_U$.

7:    **until** Convergence = **true** or $l_1^{\text{inner}} = L_{\text{max\_inner}}^{l_1}$.

8: **until** Convergence = **true** or $l_1 = L_{\text{max\_outer}}^{l_1}$.

9: $\eta^{*l_1} = \eta^{l_1}$, $\mathcal{S}_U^* = \mathcal{S}_U^{l_1}$, and $\tilde{\mathcal{P}}_U^* = \tilde{\mathcal{P}}_U^{l_1}$.

---

multipliers as shown in line 4 of **Algorithm 1**. Then, we update Lagrange multipliers via
the gradient method (34)-(37) as shown in line 6 of **Algorithm 1**.

B. Subproblem 2: Jamming Policy

In this section, we consider subproblem 2 for optimizing jamming scheduling and power
$(\mathcal{S}_J, \mathcal{P}_J)$ with the fixed communication policy and trajectories $(\mathcal{S}_U, \mathcal{P}_U, \mathcal{Q})$. Thus, subproblem
2 can be written as

$$\underset{\eta, \mathcal{S}_J, \mathcal{P}_J}{\text{maximize}} \ \eta \tag{38}$$

$$\text{s.t. C1}: \frac{1}{N}\sum_{n=1}^{N}\sum_{m=1}^{M}\sum_{i=1}^{N_\text{F}} R_{m,k_U,i}[n] - R'_{m,k_U,k_E,i}[n] \geq \eta, \forall k_U, k_E,$$

$$\text{C3}: s_{m,i}^J[n] \in \{0,1\}, \forall n, m, i,$$

$$\text{C5}: \sum_{k_U=1}^{K_\text{U}} s_{m,k_U,i}[n] + s_{m,i}^J[n] \leq 1, \forall n, m, i,$$

$$\text{C6a}: \sum_{k_U=1}^{K_\text{U}}\sum_{i=1}^{N_\text{F}} s_{m,k_U,i}[n]p_{m,k_U,i}[n] + \sum_{i=1}^{N_\text{F}} s_{m,i}^J[n]p_{m,i}^J[n] \leq P_{\text{peak}}^m, \ \forall n, m,$$

$$\text{C6c}: p_{m,i}^J[n] \geq 0, \forall n, m, i.$$

First, we handle the coupling between binary variables $s_{m,i}^J[n]$ and continuous variables
$p_{m,i}^J[n]$ in (38). We introduce an auxiliary variable $\overline{p}_{m,i}^J[n] = s_{m,i}^J[n]p_{m,i}^J[n]$ and adopt the

big-M formulation [46] to transform problem (38) equivalently as follows

$$\underset{\eta, \mathcal{S}_J, \mathcal{P}_J, \overline{\mathcal{P}}_J}{\text{maximize}} \, \eta \tag{39}$$

$$\text{s.t.} \quad \text{C3, C5, C6c,}$$

$$\overline{\text{C1}}: \frac{1}{N} \sum_{n=1}^{N} \sum_{m=1}^{M} \sum_{i=1}^{N_{\mathrm{F}}} \overline{R}_{m,k_U,i}[n] - \overline{R}'_{m,k_U,k_E,i}[n] \geq \eta, \forall k_U, k_E,$$

$$\overline{\text{C6a}}: \sum_{k_U=1}^{K_{\mathrm{U}}} \sum_{i=1}^{N_{\mathrm{F}}} s_{m,k_U,i}[n] p_{m,k_U,i}[n] + \sum_{i=1}^{N_{\mathrm{F}}} \overline{p}^J_{m,i}[n] \leq P^m_{\mathrm{peak}}, \ \forall n, m,$$

$$\text{C12}: \overline{p}^J_{m,i}[n] \geq 0, \forall n, m, i, \quad \text{C13}: \overline{p}^J_{m,i}[n] \leq p^J_{m,i}[n], \forall n, m, i,$$

$$\text{C14}: \overline{p}^J_{m,i}[n] \leq s^J_{m,i}[n] P^{Um}_{\mathrm{peak}}[n], \forall n, m, i,$$

$$\text{C15}: \overline{p}^J_{m,i}[n] \geq p^J_{m,i}[n] - (1 - s^J_{m,i}[n]) P^{Um}_{\mathrm{peak}}[n], \forall n, m, i,$$

where $\overline{\mathcal{P}}_J = \{\overline{p}^J_{m,i}[n], \forall n, m, i\}$,

$$\overline{R}_{m,k_U,i}[n] = s_{m,k_U,i}[n] \log_2 \left(1 + \frac{p_{m,k_U,i}[n] h_{m,k_U}[n]}{\overline{I}_{m,k_U,i}[n] + \sigma^2}\right), \forall n, m, k_U, i, \tag{40}$$

$$\overline{R}'_{m,k_U,k_E,i}[n] = s_{m,k_U,i}[n] \log_2 \left(1 + \frac{p_{m,k_U,i}[n] h_{m,k_E}[n]}{\overline{I}_{m,k_E,i}[n] + \sigma^2}\right), \forall n, m, k_U, k_E, i, \tag{41}$$

$$P^{Um}_{\mathrm{peak}}[n] = P^m_{\mathrm{peak}} - \sum_{k_U=1}^{K_{\mathrm{U}}} \sum_{i=1}^{N_{\mathrm{F}}} s_{m,k_U,i}[n] p_{m,k_U,i}[n], \forall n, m, \tag{42}$$

$$\overline{I}_{m,k_U,i}[n] = \sum_{m'=1,m'\neq m}^{M} \overline{p}^J_{m',i}[n] h_{m',k_U}[n], \forall n, m, k_U, i, \tag{43}$$

$$\overline{I}_{m,k_E,i}[n] = \sum_{m'=1,m'\neq m}^{M} \overline{p}^J_{m',i}[n] h_{m',k_E}[n], \forall n, m, k_E, i, \tag{44}$$

and constraints C12-C15 are imposed additionally due to the application of the big-M formulation [46]. Furthermore, the binary constraint C3 is another major obstacle for designing a computationally-efficient jamming algorithm. Therefore, the binary constraint C3 can be written in its equivalent form:

$$\text{C3a}: 0 \leq s^J_{m,i}[n] \leq 1 \quad \text{and}$$

$$\text{C3b}: \sum_{n=1}^{N} \sum_{m=1}^{M} \sum_{i=1}^{N_{\mathrm{F}}} s^J_{m,i}[n] - \sum_{n=1}^{N} \sum_{m=1}^{M} \sum_{i=1}^{N_{\mathrm{F}}} \left(s^J_{m,i}[n]\right)^2 \leq 0. \tag{45}$$

However, the optimization problem is still hard to solve due to the non-convex constraints $\overline{\text{C1}}$ and $\overline{\text{C3b}}$. Note that $\overline{\text{C1}}$ and $\overline{\text{C3b}}$ are in the form of the difference of two convex functions w.r.t. $\overline{p}^J_{m,i}[n]$ and $s^J_{m,i}[n]$, respectively [17]. Thus, following a similar approach as in [46], [47], we can augment the difference of convex (D.C.) constraints $\overline{\text{C1}}$ and $\overline{\text{C3b}}$ into the objective function with two penalty factors ζ and φ, which result in an equivalent problem.

Hence, problem (39) can be rewritten in its equivalent canonical form of D.C. programming as following

$$\underset{\eta, \mathcal{S}_J, \mathcal{P}_J, \overline{\mathcal{P}}_J}{\text{maximize}} \ F_1(\eta, \mathcal{S}_J, \overline{\mathcal{P}}_J) - F_2(\mathcal{S}_J, \overline{\mathcal{P}}_J) \tag{46}$$

$$\text{s.t.} \quad \text{C3a, C5, } \overline{\text{C6a}}, \text{C6c, C12} - \text{C15,}$$

where $F_1(\eta, \mathcal{S}_J, \overline{\mathcal{P}}_J)$ and $F_2(\mathcal{S}_J, \overline{\mathcal{P}}_J)$ are given by

$$F_1(\eta, \mathcal{S}_J, \overline{\mathcal{P}}_J) = \eta - N K_U K_E \zeta \eta - \varphi \sum_{n=1}^{N} \sum_{m=1}^{M} \sum_{i=1}^{N_{\mathrm{F}}} s_{m,i}^{J}[n] + \zeta \sum_{\Upsilon} \left[s_{m,k_E,i}[n] \log_2 \left(\overline{I}_{m,k_E,i}[n] + \sigma^2 \right) \right]$$

$$+ \zeta \sum_{\Upsilon} \left[s_{m,k_U,i}[n] \log_2 \left(\overline{I}_{m,k_U,i}[n] + \sigma^2 + p_{m,k_U,i}[n] h_{m,k_U}[n] \right) \right], \tag{47}$$

$$F_2(\mathcal{S}_J, \overline{\mathcal{P}}_J) = \zeta \sum_{\Upsilon} \left[s_{m,k_U,i}[n] \log_2 \left(\overline{I}_{m,k_E,i}[n] + \sigma^2 + p_{m,k_U,i}[n] h_{m,k_E}[n] \right) \right]$$

$$- \varphi \sum_{n=1}^{N} \sum_{m=1}^{M} \sum_{i=1}^{N_{\mathrm{F}}} \left(s_{m,i}^{J} \right)^2 [n] + \zeta \sum_{\Upsilon} \left[s_{m,k_U,i}[n] \log_2 \left(\overline{I}_{m,k_U,i}[n] + \sigma^2 \right) \right], \tag{48}$$

and we define $\sum_{\Upsilon}[\cdot]$ as $\sum_{n=1}^{N} \sum_{m=1}^{M} \sum_{k_U=1}^{K_{\mathrm{U}}} \sum_{k_E=1}^{K_{\mathrm{E}}} \sum_{i=1}^{N_{\mathrm{F}}}[\cdot]$ for notational simplicity, where $\Upsilon \triangleq \{\mathcal{N}, \mathcal{M}, \mathcal{K}_U, \mathcal{K}_E, \mathcal{N}_{\mathrm{F}}\}$. Although it is still hard to solve the non-convex problem (46) optimally, by utilizing the technique of SCA, we can obtain a locally optimal solution for problem (46) [48]. For the SCA technique, with a given feasible point at each iteration, the non-convex constraints can be approximated by the corresponding convex constraints, such that an approximated convex optimization problem can be obtained. Then, by iteratively solving the sequence of approximated convex problems, an efficient solution to the original non-convex optimization problem (38) can be obtained [48].

Note that $F_1(\eta, \mathcal{S}_J, \overline{\mathcal{P}}_J)$ and $F_2(\mathcal{S}_J, \overline{\mathcal{P}}_J)$ are differentiable concave functions w.r.t. $\eta, \mathcal{S}_J$, and $\overline{\mathcal{P}}_J$. Thus, for any feasible point $(\eta^{l_2}, \mathcal{S}_J^{l_2}, \overline{\mathcal{P}}_J^{l_2})$, we can define a global upper estimator for $F_2(\mathcal{S}_J, \overline{\mathcal{P}}_J)$ based on its first order Taylor's expansion at $(\eta^{l_2}, \mathcal{S}_J^{l_2}, \overline{\mathcal{P}}_J^{l_2})$ as follows

$$F_2(\mathcal{S}_J, \overline{\mathcal{P}_J}) \leq F_2(\mathcal{S}_J^{l_2}, \overline{\mathcal{P}}_J^{l_2}) + \nabla_{\mathcal{S}_J} F_2(\mathcal{S}_J^{l_2}, \overline{\mathcal{P}}_J^{l_2})^T (\mathcal{S}_J - \mathcal{S}_J^{l_2}) + \nabla_{\overline{\mathcal{P}}_J} F_2(\mathcal{S}_J^{l_2}, \overline{\mathcal{P}}_J^{l_2})^T (\overline{\mathcal{P}}_J - \overline{\mathcal{P}}_J^{l_2}), \tag{49}$$

where $\nabla_{\overline{\mathcal{P}}_J} F_2(\mathcal{S}_J^{l_2}, \overline{\mathcal{P}}_J^{l_2})$ and $\nabla_{\mathcal{S}_J} F_2(\mathcal{S}_J^{l_2}, \overline{\mathcal{P}}_J^{l_2})$ denote the gradient vectors of $F_2(\mathcal{S}_J, \overline{\mathcal{P}}_J)$ at $(\mathcal{S}_J^{l_2}, \overline{\mathcal{P}}_J^{l_2})$.

Moreover, the right hand side of (49) is an affine function. Thus, we can obtain a lower bound for the optimal value of problem (46) by solving the following concave maximization problem:

$$\underset{\eta, \mathcal{S}_J, \mathcal{P}_J, \overline{\mathcal{P}}_J}{\text{maximize}} F_1(\eta, \mathcal{S}_J, \overline{\mathcal{P}}_J) - F_2(\mathcal{S}_J^{l_2}, \overline{\mathcal{P}}_J^{l_2}) - \nabla_{\mathcal{S}_J} F_2(\mathcal{S}_J^{l_2}, \overline{\mathcal{P}}_J^{l_2})^T (\mathcal{S}_J - \mathcal{S}_J^{l_2}) - \nabla_{\overline{\mathcal{P}}_J} F_2(\mathcal{S}_J^{l_2}, \overline{\mathcal{P}}_J^{l_2})^T (\overline{\mathcal{P}}_J - \overline{\mathcal{P}}_J^{l_2})$$

$$\text{s.t.} \quad \text{C3a, C5, } \overline{\text{C6a}}, \text{C6c, C12} - \text{C15,} \tag{50}$$

Algorithm 2 Jamming Policy Optimization Algorithm

1: Initialize the maximum number of iterations $L_{\max}^{l_2}$, iteration index $l_2 = 0$, penalty factors ζ and φ, and the maximum tolerance ϵ^{l_2}.

2: Set the intermediate average minimum secrecy rate, jamming scheduling, jamming power, and relaxed jamming power as $\eta^{(0)}$, $\mathcal{S}_J^{(0)}$, $\mathcal{P}_J^{(0)}$, and $\overline{\mathcal{P}}_J^{(0)}$, respectively.

3: **repeat**

4:     Solve (50) for a given communication resource allocation $\{\mathcal{S}_C, \mathcal{P}_C\}$ and UAVs' trajectories $\{\mathcal{Q}\}$.

5:     Set $l_2 = l_2 + 1$, $\eta^{l_2} = \eta$, $\mathcal{S}_J^{l_2} = \mathcal{S}_J$, $\mathcal{P}_J^{l_2} = \mathcal{P}_J$, and $\overline{\mathcal{P}}_J^{l_2} = \overline{\mathcal{P}}_J$.

6: **until** convergence or $l_2 = L_{\max}^{l_2}$.

7: $\eta^{l_2} = \eta^{l_2}$, $\mathcal{S}_J = \mathcal{S}_J^{l_2}$, $\mathcal{P}_J = \mathcal{P}_J^{l_2}$, and $\overline{\mathcal{P}}_J = \mathcal{P}_J^{l_2}$.

---

where

$$\nabla_{\mathcal{S}_J} F_2(\mathcal{S}_J^{l_2}, \overline{\mathcal{P}}_J^{l_2})^T(\mathcal{S}_J - \mathcal{S}_J^{l_2}) = -2\varphi \sum_{n=1}^{N} \sum_{m=1}^{M} \sum_{i=1}^{N_F} s_{m,i}^{J(l_2)}[n]\left(s_{m,i}^J[n] - s_{m,i}^{J(l_2)}[n]\right), \tag{51}$$

$$\nabla_{\overline{\mathcal{P}}_J} F_2(\mathcal{S}_J^{l_2}, \overline{\mathcal{P}}_J^{l_2})^T(\overline{\mathcal{P}}_J - \overline{\mathcal{P}}_J^{l_2}) = \zeta \sum_{\Upsilon}\left[\frac{s_{m,k_U,i}[n]}{\ln 2}\left(A_{m,k_U,i}^{l_2}[n] + B_{m,k_U,k_E,i}^{l_2}[n]\right)\left(\overline{p}_{m,i}^J[n] - \overline{p}_{m,i}^{J(l_2)}[n]\right)\right], \tag{52}$$

$$A_{m,k_U,i}^{l_2}[n] = \frac{\sum\limits_{m'=1,m'\neq m}^{M} h_{m',k_U}[n]}{\overline{I}_{m,k_U,i}^{l_2}[n] + \sigma^2}, \tag{53}$$

$$B_{m,k_U,k_E,i}^{l_2}[n] = \frac{\sum\limits_{m'=1,m'\neq m}^{M} h_{m',k_E}[n]}{\overline{I}_{m,k_E,i}^{l_2}[n] + \sigma^2 + p_{m,k_U,i}[n]h_{m,k_E}[n]}. \tag{54}$$

Now, the optimization problem in (50) is a convex optimization problem which can be solved efficiently by standard convex problem solvers, such as CVX [42]. To tighten the obtained lower bound, we adopt an iterative algorithm to generate a sequence of feasible solutions successively, cf. **Algorithm 2**. The initial feasible solution with iteration index $l_2 = 0$ is obtained by solving the convex optimization problem in (50) with $F_1(\eta, \mathcal{S}_J, \overline{\mathcal{P}}_J)$ as the objective function [46] which is shown in line 2 of **Algorithm 2**. Then, the intermediate solution from the last iteration will be used to update the problem in (50) and it will generate a feasible solution for the next iteration in $l_2 = l_2 + 1$, as shown in line 5 of **Algorithm 2**. The iterative procedure will stop either the changes of optimization variables are smaller than a predefined convergence tolerance or the number of iteration reaches its maximum.

C. Subproblem 3: Trajectory Optimization

In this section, we consider subproblem 3 for optimizing the trajectory design by assuming that $(\mathcal{S}_U, \mathcal{S}_J, \mathcal{P}_U, \mathcal{P}_J)$ are fixed. Thus, subproblem 3 can be written as

$$\underset{\eta, \mathcal{Q}}{\text{maximize}} \ \eta \tag{55}$$

$$\text{s.t. C1}: \frac{1}{N}\sum_{n=1}^{N}\sum_{m=1}^{M}\sum_{i=1}^{N_F} R_{m,k_U,i}[n] - R'_{m,k_U,k_E,i}[n] \geq \eta, \forall k_U, k_E,$$

$$\text{C7}: ||\mathbf{q}_m[n] - \mathbf{q}_m[n-1]||^2 \leq V^2, \forall n, m,$$

$$\text{C8}: ||\mathbf{q}_m[n] - \mathbf{w}_{\text{NF}}^j||^2 \geq \left(Q_{\text{NF}}^j\right)^2, \forall n, m, j,$$

$$\text{C9}: ||\mathbf{q}_m[n] - \mathbf{q}_{m'}[n]||^2 \geq D_S^2, \forall n, m, m \neq m',$$

$$\text{C10}: \mathbf{q}_m[0] = \mathbf{q}_m^0, \forall m, \qquad\qquad \text{C11}: \mathbf{q}_m[N] = \mathbf{q}_m^F, \forall m.$$

However, the optimization problem is still non-convex due to constraints C1, C8, and C9. To facilitate the development of solution, we first introduce four slack variables $\mathbf{t}_U = \{t_{m,k_U}[n], \forall n, m, k_U\}$, $\mathbf{t}'_U = \{t'_{m,k_U}[n], \forall n, m, k_U\}$, $\mathbf{t}_E = \{t_{m,k_E}[n], \forall n, m, k_E\}$, and $\mathbf{t}'_E = \{t'_{m,k_E}[n], \forall n, m, k_E\}$, which satisfy

$$\text{C12}: \ t_{m,k_U}[n] \geq d_{m,k_U}^2[n], \forall n, m, k_U, \quad \text{C13}: \ t_{m,k_E}[n] \geq d_{m,k_E}^2[n], \forall n, m, k_E, \tag{56}$$

$$\text{C14}: \ t'_{m,k_U}[n] \leq d_{m,k_U}^2[n], \forall n, m, k_U, \quad \text{C15}: \ t'_{m,k_E}[n] \leq d_{m,k_E}^2[n], \forall n, m, k_E. \tag{57}$$

Then, communication rate $R_{m,k_U,i}[n]$ in constraint C1 can be written as

$$R_{m,k_U,i}[n] = s_{m,k_U,i}[n] \log_2\left(1 + \frac{\frac{p_{m,k_U,i}[n]\beta_0}{t_{m,k_U}[n]}}{\Omega_{m,k_U}[n]}\right) = \hat{R}_{m,k_U,i}[n] - \check{R}_{m,k_U,i}[n], \forall n, m, k_U, i, \tag{58}$$

where

$$\hat{R}_{m,k_U,i}[n] = s_{m,k_U,i}[n] \log_2\left(\frac{p_{m,k_U,i}[n]\beta_0}{t_{m,k_U}[n]} + \Omega_{m,k_U}[n]\right), \tag{59}$$

$$\check{R}_{m,k_U,i}[n] = s_{m,k_U,i}[n] \log_2 \Omega_{m,k_U}[n], \tag{60}$$

$$\Omega_{m,k_U}[n] = \sum_{m'=1,m'\neq m}^{M} \frac{s_{m',i}^J[n]p_{m',i}^J[n]\beta_0}{t'_{m,k_U}[n]} + \sigma^2. \tag{61}$$

Similarly, the leakage rate in constraint C1 can be written as

$$R'_{m,k_U,k_E,i}[n] = s_{m,k_U,i}[n]\log_2\left(1 + \frac{\frac{p_{m,k_U,i}[n]\beta_0}{t_{m,k_E}[n]}}{\Omega_{m,k_E}[n]}\right) = \check{R}'_{m,k_U,k_E,i}[n] - \hat{R}'_{m,k_U,k_E,i}[n], \forall n, m, k_U, k_E, i, \tag{62}$$

where

$$\check{R}'_{m,k_U,k_E,i}[n] = s_{m,k_U,i}[n]\log_2\left(\frac{p_{m,k_U,i}[n]\beta_0}{t_{m,k_E}[n]} + \Omega_{m,k_E}[n]\right), \tag{63}$$

$$\hat{R}'_{m,k_U,k_E,i}[n] = s_{m,k_U,i}[n]\log_2\Omega_{m,k_E}[n], \tag{64}$$

$$\Omega_{m,k_E}[n] = \sum_{m'=1,m'\neq m}^{M} \frac{s^J_{m',i}[n]p^J_{m',i}[n]\beta_0}{t'_{m,k_E}[n]} + \sigma^2. \tag{65}$$

Therefore, the problem can be written as

$$\underset{\eta,\mathcal{Q},\mathbf{t}_U,\mathbf{t}_E,\mathbf{t}'_U,\mathbf{t}'_E}{\text{maximize}} \quad \eta \tag{66}$$

s.t. C7 − C11,

$$\hat{C}1: \quad \frac{1}{N}\sum_{n=1}^{N}\sum_{m=1}^{M}\sum_{i=1}^{N_F} \hat{R}_{m,k_U,i}[n] + \hat{R}'_{m,k_U,k_E,i}[n] - \check{R}_{m,k_U,i}[n] - \check{R}'_{m,k_U,k_E,i}[n] \geq \eta, \forall k_U, k_E,$$

C12 : $t_{m,k_U}[n] \geq d^2_{m,k_U}[n], \forall n, m, k_U,$ C13 : $t_{m,k_E}[n] \geq d^2_{m,k_E}[n], \forall n, m, k_E,$

C14 : $t'_{m,k_U}[n] \leq d^2_{m,k_U}[n], \forall n, m, k_U,$ C15 : $t'_{m,k_E}[n] \leq d^2_{m,k_E}[n], \forall n, m, k_E,$

where $\mathbf{t}_U = \{t_{m,k_U}[n], \forall n, m, k_U\}$, $\mathbf{t}_E = \{t_{m,k_E}[n], \forall n, m, k_E\}$, $\mathbf{t}'_U = \{t'_{m,k_U}[n], \forall n, m, k_U\}$, and $\mathbf{t}'_E = \{t'_{m,k_E}[n], \forall n, m, k_E\}$.

Since $\hat{R}_{m,k_U,i}[n]$, $\check{R}_{m,k_U,i}[n]$, $\hat{R}'_{m,k_U,k_E,i}[n]$, and $\check{R}'_{m,k_U,k_E,i}[n]$ are convex functions w.r.t. $t_{m,k_U}[n]$, $t'_{m,k_U}[n]$, $t_{m,k_E}[n]$, and $t'_{m,k_E}[n]$, respectively, problem (66) is equivalent to problem (55), as constraints C12 - C15 hold with equalities at the optimal point of problem (66) [1], [18].

However, problem (66) is still non-convex due to the non-convex constraints $\hat{C}1$, C8, C9, C14, C15, C16, and C18. Although it is hard to solve the non-convex problem (66) optimally, similar to the case for solving subproblem 2, by utilizing the technique of SCA, we can obtain a locally optimal solution for problem (66). To this end, we first handle constraint $\hat{C}1$. Since $-\check{R}_{m,k_U,i}[n]$ is a convex functions w.r.t. $\{t'_{m,k_U}[n]\}$. We have the following inequalities by applying the first order Taylor expansion at any given point $\{t'_{m,k_U}[n]\}$

$$-\check{R}_{m,k_U,i}[n] = -s_{m,k_U,i}[n]\log_2\Omega_{m,k_U}[n]$$

$$\geq -\check{R}^{l_3}_{m,k_U,i}[n] - \nabla_{t'_U}\check{R}^{l_3}_{m,k_U,i}[n]\left(t'_{m,k_U}[n] - t'^{l_3}_{m,k_U}[n]\right)$$

$$\triangleq -\check{R}^{lb}_{m,k_U,i}[n], \forall n, m, k_U, i, \tag{67}$$

where

$$\check{R}^{l_3}_{m,k_U,i}[n] = s_{m,k_U,i}[n]\log_2\Omega^{l_3}_{m,k_U}[n], \tag{68}$$

$$\nabla_{t'_U}\check{R}^{l_3}_{m,k_U,i}[n] = -\sum_{m'=1,m'\neq m}^{M}\frac{s_{m,k_U,i}[n]s^J_{m',i}[n]p^J_{m',i}[n]\beta_0}{\left(t'^{l_3}_{m',k_U}[n]\right)^2\Omega^{l_3}_{m,k_U}[n]\ln 2}. \tag{69}$$

Similarly, we approximate $-\check{R}'_{m,k_U,k_E,i}[n]$ by applying the first order Taylor expansion at given points $\{t_{m,k_E}[n]\}$ and $\{t'_{m,k_E}[n]\}$

$$-\check{R}'_{m,k_U,k_E,i}[n] = -s_{m,k_U,i}[n]\log_2\left(\frac{p_{m,k_U,i}[n]\beta_0}{t_{m,k_E}[n]} + \Omega^{l_3}_{m,k_E}[n]\right)$$

$$\geq -\check{R}'^{l_3}_{m,k_U,k_E,i}[n] - \nabla_{t_E}\check{R}'^{l_3}_{m,k_U,k_E,i}[n]\left(t_{m,k_E}[n] - t^{l_3}_{m,k_E}[n]\right) - \nabla_{t'_E}\check{R}'^{l_3}_{m,k_U,k_E,i}[n]\left(t'_{m,k_E}[n] - t'^{l_3}_{m,k_E}[n]\right)$$

$$\triangleq -\check{R}^{\text{lb}}_{m,k_U,k_E,i}[n], \forall n, m, k_U, k_E, i, \tag{70}$$

where

$$\check{R}'^{l_3}_{m,k_U,k_E,i}[n] = s_{m,k_U,i}[n]\log_2\left(\frac{p_{m,k_U,i}[n]\beta_0}{t^{l_3}_{m,k_E}[n]} + \Omega^{l_3}_{m,k_E}[n]\right), \tag{71}$$

$$\nabla_{t_E}\check{R}'^{l_3}_{m,k_U,k_E,i}[n] = \frac{-s_{m,k_U,i}[n]p_{m,k_U,i}[n]\beta_0}{\left(t^{l_3}_{m,k_E}[n]\right)^2\left(\frac{p_{m,k_U,i}[n]\beta_0}{t^{l_3}_{m,k_E}[n]} + \Omega^{l_3}_{m,k_E}[n]\right)\ln 2}, \tag{72}$$

$$\nabla_{t'_E}\check{R}'^{l_3}_{m,k_U,k_E,i}[n] = \sum_{m'=1,m'\neq m}^{M} \frac{-s_{m,k_U,i}[n]s^{J}_{m',i}[n]p^{J}_{m',i}[n]\beta_0}{\left(t'^{l_3}_{m',k_E}[n]\right)^2\left(\frac{p_{m,k_U,i}[n]\beta_0}{t^{l_3}_{m,k_E}[n]} + \Omega^{l_3}_{m,k_E}[n]\right)\ln 2}. \tag{73}$$

By replacing $-\check{R}_{m,k_U,i}[n] - \check{R}'_{m,k_U,k_E,i}[n]$ in $\hat{C}1$, constraint $\hat{C}1$ can be written as

$$\hat{\hat{C}}1 : \frac{1}{N}\sum_{n=1}^{N}\sum_{m=1}^{M}\sum_{i=1}^{N_F}\hat{R}_{m,k_U,i}[n] + \hat{R}'_{m,k_U,k_E,i}[n] - \check{R}^{\text{lb}}_{m,k_U,i}[n] - \check{R}^{\text{lb}}_{m,k_U,k_E,i}[n] \geq \eta, \forall k_U, k_E. \tag{74}$$

Then, we handle the non-convex NFZ constraint C8

$$\hat{C}8 : ||\mathbf{q}^{l_3}_m[n] - \mathbf{w}^{j}_{\text{NF}}||^2 + 2\left(\mathbf{q}^{l_3}_m[n] - \mathbf{w}^{j}_{\text{NF}}\right)\left(\mathbf{q}_m[n] - \mathbf{q}^{l_3}_m[n]\right) \geq \left(Q^{j}_{\text{NF}}\right)^2, \forall n, m, j. \tag{75}$$

Similarly, we approximate the non-convex constraint C9, C14, and C15 as following

$$\hat{C}9 : ||\mathbf{q}^{l_3}_m[n] - \mathbf{q}^{l_3}_{m'}[n]||^2 + 2\left(\mathbf{q}^{l_3}_m[n] - \mathbf{q}^{l_3}_{m'}[n]\right)\left(\mathbf{q}_m[n] - \mathbf{q}^{l_3}_m[n]\right) \geq D^2_{\text{S}}, \forall n, m, m' \neq m, \tag{76}$$

$$\hat{C}14 : ||\mathbf{q}^{l_3}_m[n] - \mathbf{w}_{k_U}||^2 + 2\left(\mathbf{q}^{l_3}_m[n] - \mathbf{w}_{k_U}\right)\left(\mathbf{q}_m[n] - \mathbf{q}^{l_3}_m[n]\right) + H^2 \geq t'_{m,k_U}[n], \forall n, m, k_U, \tag{77}$$

$$\hat{C}15 : ||\mathbf{q}^{l_3}_m[n] - \mathbf{w}_{k_E}||^2 + 2\left(\mathbf{q}^{l_3}_m[n] - \mathbf{w}_{k_E}\right)\left(\mathbf{q}_m[n] - \mathbf{q}^{l_3}_m[n]\right) + H^2 \geq t'_{m,k_E}[n], \forall n, m, k_E. \tag{78}$$

Now, with the more stringent constraints $\hat{\hat{C}}1$, $\hat{C}8$, $\hat{C}9$, $\hat{C}14$, and $\hat{C}15$, a suboptimal solution of (55) can be obtained by solving the following optimization problem

$$\underset{\eta,\mathcal{Q},\mathbf{t}_U,\mathbf{t}_E,\mathbf{t}'_U,\mathbf{t}'_E}{\text{maximize}} \quad \eta \tag{79}$$

$$\text{s.t.} \quad \hat{\hat{C}}1, C7, \hat{C}8, \hat{C}9, C10 - C13, \hat{C}14, \hat{C}15,$$

which is a convex optimization problem and can be solved efficiently by standard convex problem solvers such as CVX [42], which is summarized in **Algorithm 3**.

Algorithm 3 Trajectory Design Optimization Algorithm

1: Initialize the maximum number of iterations $L_{\max}^{l3}$, iteration index $l^{l3} = 0$, and the maximum tolerance ϵ^{l3}.

2: Set the initial values as $\eta^{(0)}$, $\mathcal{Q}^{(0)}$, $\mathbf{t}_U^{(0)}$, $\mathbf{t}_E^{(0)}$, $\mathbf{t}'^{(0)}_U$, and $\mathbf{t}'^{(0)}_E$, respectively.

3: **repeat**

4:     Solve (79) for a given communication resource allocation $\{\mathcal{S}_C, \mathcal{P}_C\}$ and jammer policy $\{\mathcal{S}_J, \mathcal{P}_J\}$.

5:     Set $l_3 = l_3 + 1$, $\eta^{l3} = \eta$, $\mathcal{Q}^{l3} = \mathcal{Q}$, $\mathbf{t}_U^{l3} = \mathbf{t}_U$, $\mathbf{t}_E^{l3} = \mathbf{t}_E$, $\mathbf{t}'^{l3}_U = \mathbf{t}'_U$, and $\mathbf{t}'^{l3}_E = \mathbf{t}'_E$.

6: **until** convergence or $l_3 = L_{\max}^{l3}$.

7: $\eta^{l3} = \eta^{l3}$, $\mathcal{Q} = \mathcal{Q}^{l3}$, $\mathbf{t}_U = \mathbf{t}_U^{l3}$, $\mathbf{t}_E = \mathbf{t}_E^{l3}$, $\mathbf{t}'_E = \mathbf{t}'^{l3}_U$, and $\mathbf{t}'_E = \mathbf{t}'^{l3}_E$.

Algorithm 4 Iterative Resource Allocation and Trajectory Optimization Algorithm

---

1: Initialize the maximum number of iterations $L_{\max}^{l4}$, iteration index $l_4 = 0$, and the maximum tolerance ϵ^{l4}.

2: **repeat**

3:     For the fixed jamming policy and trajectory, obtain the optimal communication resource allocation $\{\mathcal{S}_U^*, \mathcal{P}_U^*\}$ and intermediate average minimum secrecy rate η^{l_1} by using Algorithm 1.

4:     For the fixed communication resource allocation and trajectory, obtain the jamming policy $\{\mathcal{S}_J, \mathcal{P}_J\}$ and intermediate average minimum secrecy rate η^{l_2} by using Algorithm 2.

5:     For the fixed communication resource allocation and jamming policy, obtain the trajectory $\mathcal{Q}$ and intermediate average minimum secrecy rate η^{l_3} by using Algorithm 3.

6:     Set $l_4 = l_4 + 1$, $\eta^{l4} = \eta^{l3}$, $\{\mathcal{S}_U^{l4}, \mathcal{P}_U^{l4}\} = \{\mathcal{S}_U^*, \mathcal{P}_U^*\}$, $\{\mathcal{S}_J^{l4}, \mathcal{P}_J^{l4}\} = \{\mathcal{S}_J, \mathcal{P}_J\}$, and $\mathcal{Q}^{l4} = \mathcal{Q}$.

7: **until** convergence or iteration index reaches to the maximum number.

8: $\eta = \eta^{l4}$, $\{\mathcal{S}_U, \mathcal{P}_U\} = \{\mathcal{S}_U^{l4}, \mathcal{P}_U^{l4}\}$, $\{\mathcal{S}_J, \mathcal{P}_J\} = \{\mathcal{S}_J^{l4}, \mathcal{P}_J^{l4}\}$, and $\mathcal{Q} = \mathcal{Q}^{l4}$.

D. Overall Algorithm

In summary, the proposed algorithm solves the three subproblems (20), (38), and (55) in an alternating manner with a polynomial time computational complexity. The details of the proposed algorithm are summarized in **Algorithm 4**. Since the objective value of (18) with the solutions obtained by solving subproblems (20), (38), and (55) is non-decreasing over iterations and feasible solution set is bounded, the solution obtained by the proposed algorithm is guaranteed to converge to a suboptimal solution with a polynomial time computational complexity [7], [46].

V. NUMERICAL RESULTS

In this section, we investigate the performance of the proposed UAV-enabled secure communication scheme through simulations. Unless specified otherwise, the system parameters are given as follows. All ground users are placed on the ground within the area of 500×500 m^2. Two UAVs are dispatched to provide communications to two ground users with the existence with two potential eavesdroppers. Furthermore, we assume that the two UAVs' initial locations and final locations in 2D area are $\mathbf{q}_1^0 = (0, 0)$, $\mathbf{q}_1^F = (500, 0)$, $\mathbf{q}_2^0 = (0, 500)$, and $\mathbf{q}_2^F = (500, 500)$, respectively. The communication bandwidth is 2 MHz with a carrier center frequency at 2 GHz, the number of subcarrier $N_F = 16$, and the noise power on each subcarrier is -100 dBm with channel gain $\beta_0 = -50$ dB at the reference distance $d_0 = 1$ m. Therefore, the channel gain-to-noise ratio at the reference distance is $\gamma_0 = 80$
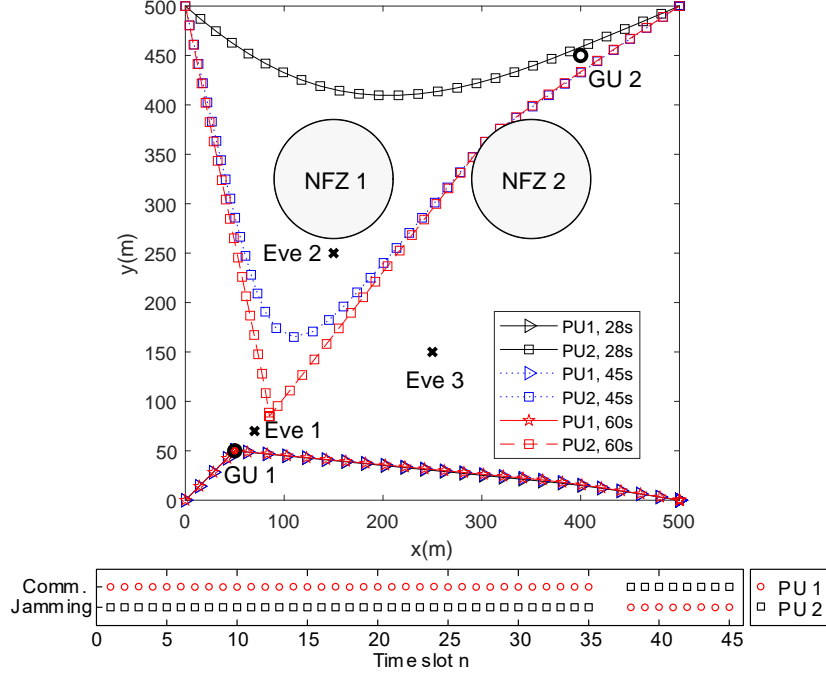
Fig. 3. The upper half of the figure shows the proposed algorithm trajectories with different mission time durations. The lower half of the figure depicts the roles of the two UAVs for the case of $T = 45$ s.

dB [18]. All UAVs' maximum transmission power are set as $P_{\text{peak}} = 30$ dBm [20]. Both of the UAV's maximum flying speed is $v_{\text{max}} = 20$ m/s with a fixed altitude of $H = 100$ m, and the safety distance between any two UAVs is $D_{\text{S}} = 50$ m. The centres of two NFZs are $\mathbf{w}_{\text{NF}}^1 = (150, 325)$ and $\mathbf{w}_{\text{NF}}^2 = (350, 325)$, respectively, and the radii of both NFZs are the same with $Q_{\text{NF}} = 60$ m. In all considered scenarios, two users are located on $\mathbf{w}_{k1_U} = (50, 50)$ and $\mathbf{w}_{k2_U} = (400, 450)$, respectively. Furthermore, as in [8], [17], [18], we assume that three eavesdroppers' locations are exactly known as $\mathbf{w}_{1_E} = (70, 70)$, $\mathbf{w}_{2_E} = (150, 250)$, and $\mathbf{w}_{3_E} = (250, 150)$. For illustration, all the trajectories are sampled every second.

In our simulation, we compare the performance of the proposed algorithm, denoted as PA with the other two baseline schemes: a) *No jammer (NJ)*, which all UAVs serve as information UAV and do not transmit artificial noise to eavesdroppers [14]–[16]. Since the problem for PA subsumes the NJ scheme as a subcase, the average minimum secrecy rate per user in NJ can be achieved by solving subproblem 1 and subproblem 3 with the settings of jamming power as zero. (b) *Single-purpose UAV (SP)*, which one UAV can provide communication while the other is acting as a jammer at all time [17], [18], [20]. SP is also a subcase for PA, and the average minimum secrecy rate in PA can be obtained by solving the problem in (18) with fixing UAV 1 as a jammer and UAV 2 as a base station.

A. Proposed Trajectories with Different Mission Time Durations

Fig. 3 illustrates UAVs' trajectories of our proposed scheme with three different mission time durations, $T = 28$ s, $T = 45$ s, and $T = 60$ s, respectively. The proposed trajectories in this figure for UAV 1 and UAV 2 are denoted as PU 1 and PU 2, respectively. It is observed that when T is relatively small (e.g. $T = 28$ s), UAV 1 first goes directly towards ground user 1 (GU 1) and hovers over it before flying back straightly to the destination, whereas the behavior of UAV 2 is totally different. This is because all three eavesdroppers are closer to GU 1 compared to GU 2. Specifically, eavesdropper 1 is in close proximity to GU 1 which incurs a high risk in information leakage. Therefore, UAV 2 first acts as a jammer and flies close to all the eavesdroppers as possible at the beginning to help UAV 1 for secure communications. After UAV 1 conveys enough secure data to GU 1, UAV 1 switches its role to a jamming UAV while on its way back to its final location. Concurrently, to achieve fairness in resource allocation, UAV 2 flies towards GU 2 and transmits information to GU 2 when they are close enough to each other. In addition, both UAVs fly with the maximum speed $v_{\max} = 20$ m/s to establish a shorter LoS link to the user/eavesdropper as fast as possible. Moreover, we can observe that with a sufficiently long time duration (e.g. $T = 45$ s), the behaviors of the UAVs alter to fully exploit the degrees of freedom brought by the additional time. For the ease of illustration, the lower half of Fig. 3 shows the roles of UAVs across time for the case of $T = 45$ s. In particular, for $n \leq 35$, UAV 2 first cruises towards eavesdropper 1 and serves as a jammer to assist the secure communications between UAV 1 and GU 1. Besides, with the help of UAV 2, UAV 1 also takes the shortest path cruising towards GU 1 and hovers over it for efficient communication. From $35 < n < 38$, both UAVs prepare role switching by navigating themselves to their desired positions. During this short period of time, the channels between UAVs and any of the eavesdroppers are better than that of all users even if jamming is performed. To prevent information leakage, both UAVs would not communicate to any ground user, as revealed in Lemma 3. Therefore, there is neither communication nor jamming in the system in this period. Furthermore, when UAV 2 is close enough to GU 2 for efficient secure communication at $n \geq 38$, UAV 1 starts serving as a jammer on its journey to final destination to protect GU 2 against eavesdropping. It is also observed that when the straight direction between a UAV and the desired location is blocked by a NFZ, the UAV's trajectory of the proposed scheme would take the shortest path along the tangential line of the NFZ. Also, the roles of both the UAVs remain the same before cruising back to their corresponding destinations. We can also observe that when the mission time duration is sufficiently long (e.g. $T = 60$ s), UAV 2 would spend more time
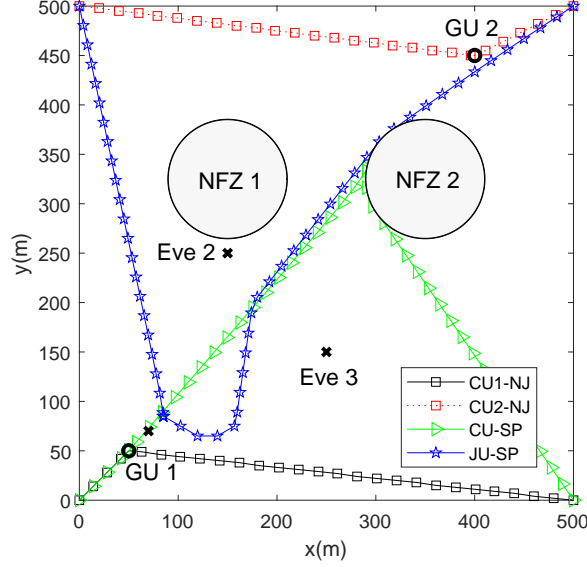
Fig. 4. Trajectories of single-purpose UAVs for different schemes.

and hover over at some locations close to eavesdropper 1 to fully exploit the additional time as a jammer for efficient jamming. Moreover, UAV 2 keeps safety distance with UAV 1 and there is no collision between them thanks to the collision avoidance constraint C9 in the problem formulation.

B. Baseline Trajectories with Fixed Mission Duration Time

Fig. 4 shows the trajectories of a single-purpose UAV system for a mission duration time of $T = 60$ s. For baseline 1 (NJ), the trajectories of communication UAV 1 and communication UAV 2 are denoted as CU1-NJ and CU2-NJ, respectively. For baseline 2 (SP), the trajectories of communication UAV and jammer UAV are denoted as CU-SP and JU-SP, respectively. It can be observed that for baseline 1, UAV 1 and UAV 2 fly directly to GU 1 and GU 2 with the maximum speed $v_{max} = 20$ m/s, respectively. Besides, each UAV hovers over their corresponding desired GU as long as possible within the allowed mission duration time. Then, both of the UAVs fly directly to the final location. Different from baseline 1, the single purpose communication UAV CU-SP in baseline 2 just hovers over GU 1 for a short period duration time and then flies directly to GU 2 from the left hand side of NFZ 2 for establishing efficient communication between them. This is because CU-SP needs to fly towards and communicate to a far away user, i.e., GU 2, even if another single-purpose jamming UAV JU-SP is closer to this remote user. In this scheme, the only communication UAV has no choice but fly closer to the desired user to establish a strong LoS link to provide secure communication. At the same time, the JU-SP UAV flies close to eavesdropper 1 for jamming at the beginning to relieve the system bottleneck created by eavesdropper 1. Then,
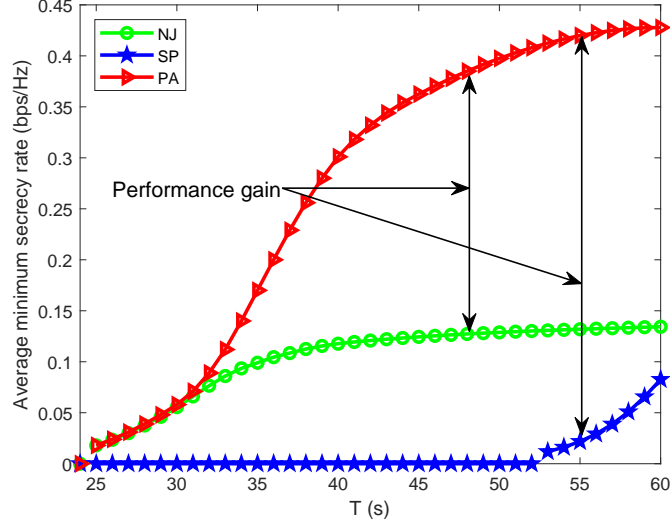
Fig. 5. Average minimum secrecy rate versus the mission time durations with different schemes.

the JU-SP UAV flies close to the centroid location formed by the three eavesdroppers to improve secrecy rate communication. In particular, to avoid UAVs collision, JU-SP moves away from its hovering location to give way for CU-SP. This is because in baseline 2, there is only one communication UAV for serving all users which imposes a very stringent restriction in utilizing the system resources for maximizing the average minimum secrecy rate.

C. Average Minimum Secrecy Rate versus Mission Duration Time

Fig. 5 depicts the average minimum secrecy rate versus the mission duration time T for our proposed algorithm and the other two baselines with three eavesdroppers. It is observed that for all the considered algorithms, the average minimum secrecy rate is virtually zero when the mission time duration is less than 25 s. In fact, a small time duration would lead to an infeasible result for all the algorithms, since both the UAVs cannot fly back to their final locations even if there is no NFZ and they cruise with the maximum aviation speed $v_{\max} = 20$ m/s. Also, it can be observed that the average minimum secrecy rates achieved by PA and NJ both increase with mission duration time T. However, for SP, the average minimum secrecy rate is zero until the mission duration time T is longer than 53 s. This is because the only communication UAV in SP has insufficient time to reach closer to GU 2 and to provide secure communication. As a result, the UAV would not transmit anything to avoid information leakage, as revealed in Lemma 3. Furthermore, we can observe that the system performance of PA increases sharply from 30 s to 40 s while the average minimum secrecy rate of NJ scales up slowly. In fact, a sufficiently long time duration grants a UAV more time to reach and stay close to its desired location to enjoy a short distance communication. Besides, the proposed role switching for UAVs grants the UAVs much higher flexibility to
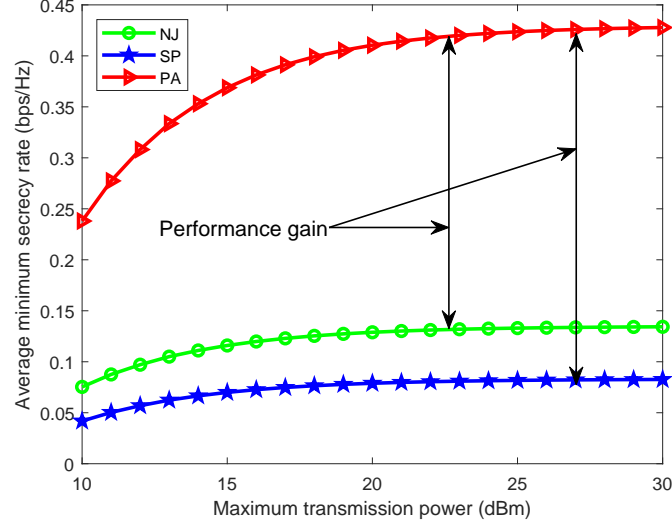
Fig. 6. Average minimum secrecy rate versus the maximum transmission power with different schemes.

provide communication or to act as a jammer, which can save considerable time for the UAVs to fly to their desired destinations. However, the system performance gain brought by the extra time is diminishing for both PA and NJ. In other words, for a given maximum transmit power, the performance bottleneck created by limited time duration is relieved as each GU can be served with a sufficiently long time while enjoying excellent channel conditions with UAVs.

D. Average Minimum Secrecy Rate versus Maximum Transmission Power

Fig. 6 demonstrates the achieved average minimum secrecy rate versus the maximum transmission power for all schemes for $T = 60$ s. It can be observed that the average minimum secrecy rates achieved by all schemes increase with the maximum transmission power at the beginning. Indeed, a higher data rate can be achieved with a higher power when the UAVs are close to their desired users. However, the system performance of all three algorithms is saturated when the maximum transmission power is sufficiently high. This is because eavesdropper 1 is in the neighbourhood of GU 1, a higher transmission power may incur a higher information leakage and the UAV would clip its transmit power at a certain level despite there is still transmit power available. Moreover, it is interesting to see that the performance gain achieved by our proposed algorithm PA are quite large at all times compared to other two baselines which unveils that role switching among UAVs is the key for improving the system performance. In addition, the average minimum secrecy rate of both SP and NJ schemes scale slowly w.r.t. the available power compared to the proposed scheme as they are less efficient in exploiting the extra transmission power for improving the system performance. Also, despite a higher maximum transmission power grants all UAVs

higher capabilities to improve secure communication system performance, single-purpose UAVs perform the worst among all the considered schemes as they are not competent for time-critical mission in secure communication systems due to the distributed nature of GUs.

VI. Conclusion

In this paper, we presented a new communication approach with multi-purpose UAVs which can either provide communication to users or serve as jammers to transmit noise signal to eavesdroppers. By exploiting the UAVs' high mobility, we maximize the average minimum secrecy rate by jointly optimizing the communication user scheduling, communication power allocation, jamming policy, and the trajectories of UAVs, while taking into account the safety distance between any two UAVs, restricted flight in NFZs, the maximum UAV cruising speed, and initial/final UAV locations. A suboptimal solution of resource allocation for secure multi-UAV communication systems was derived by utilizing dual decomposition and SCA with a polynomial time computational complexity. Numerical results demonstrated that our proposed design of multi-purpose UAV communication system can significantly increase the minimum secrecy data rate compared to various baseline schemes enabled by dynamically switching the roles of UAVs between communication and jamming.

Appendix

A. Proof of Lemma 1

Denote η_1^* and η_2^* as the optimal values of problems (18) and (19), respectively. Since $[x]^+ \geq x, \forall x$, we have $\eta_1^* \geq \eta_2^*$.

Next, we prove that $\eta_2^* \geq \eta_1^*$ holds either. Denote $(\mathcal{Q}^*, \mathcal{S}_U^*, \mathcal{S}_J^*, \mathcal{P}_U^*, \mathcal{P}_J^*)$ as the optimal solution to (18), where $\mathcal{P}_U^* = \{p_{m,k_U,i}^*[n], \forall n, m, k_U, i\}$. Define $f(p_{m,k_U,i}[n]) = R_{m,k_U,i}[n] - R'_{m,k_U,k_E,i}[n]$. We construct a feasible solution $(\hat{\mathcal{Q}}, \hat{\mathcal{S}}_U, \hat{\mathcal{S}}_J, \hat{\mathcal{P}}_U, \hat{\mathcal{P}}_J)$ to (19), such that $\hat{\mathcal{Q}} = \mathcal{Q}^*$, $\hat{\mathcal{S}}_U = \mathcal{S}_U^*$, $\hat{\mathcal{S}}_J = \mathcal{S}_J^*$, $\hat{\mathcal{P}}_J = \mathcal{P}_J^*$, and the elements of $\hat{\mathcal{P}}_U$ can be obtained as: if $f(p_{m,k_U,i}[n]) \geq 0$, $\hat{P}_{m,k_U,i}[n] = P_{m,k_U,i}^*[n]$; otherwise $\hat{P}_{m,k_U,i}[n] = 0$. Denote $\hat{\eta}$ as the objective value of (19) attained at $\hat{\mathcal{Q}}, \hat{\mathcal{S}}_U, \hat{\mathcal{S}}_J, \hat{\mathcal{P}}_U, \hat{\mathcal{P}}_J$. Therefore, the newly constructed solution $(\hat{\mathcal{Q}}, \hat{\mathcal{S}}_U, \hat{\mathcal{S}}_J, \hat{\mathcal{P}}_U, \hat{\mathcal{P}}_J)$ ensures $\hat{\eta} = \eta_1^*$, but also is feasible to (19), which follows that $\eta_2^* \geq \hat{\eta}$ and thus $\eta_2^* \geq \eta_1^*$. Therefore, $\eta_2^* = \eta_1^*$, which completes the proof.

B. Proof of Lemma 2

The Hessian of $\psi(x,y) \triangleq x \log_2(1 + \frac{\kappa_1 y}{x}) - x \log_2(1 + \frac{\kappa_2 y}{x})$ is given by

$$\bigtriangledown^2 \psi(x,y) = \begin{bmatrix} \frac{\kappa_2^2 y^2}{x^3(\frac{\kappa_2 y}{x}+1)^2} - \frac{\kappa_1^2 y^2}{x^3(\frac{\kappa_1 y}{x}+1)^2} & \frac{\kappa_1^2 y}{x^2(\frac{\kappa_1 y}{x}+1)^2} - \frac{\kappa_2^2 y}{x^2(\frac{\kappa_2 y}{x}+1)^2} \\ \frac{\kappa_1^2 y}{x^2(\frac{\kappa_1 y}{x}+1)^2} - \frac{\kappa_2^2 y}{x^2(\frac{\kappa_2 y}{x}+1)^2} & \frac{\kappa_2^2}{x(\frac{\kappa_2 y}{x}+1)^2} - \frac{\kappa_1^2}{x(\frac{\kappa_1 y}{x}+1)^2} \end{bmatrix}. \tag{80}$$

For any $\mathbf{t} = [t_1, t_2]^T$, we have

$$\mathbf{t}^T \bigtriangledown^2 \psi(x,y)\mathbf{t} = -\frac{1}{x}\left(\frac{t_1 y^2}{x} - t_2\right)^2 \left(\frac{\kappa_1^2}{\left(\frac{\kappa_1 y}{x}+1\right)^2} - \frac{\kappa_2^2}{\left(\frac{\kappa_2 y}{x}+1\right)^2}\right). \qquad (81)$$

It is easy to verify that, for $\kappa_1 > \kappa_2 \geq 0$, $x \geq 0$, and $y \geq 0$,

$$\frac{\kappa_1^2}{\left(\frac{\kappa_1 y}{x}+1\right)^2} - \frac{\kappa_2^2}{\left(\frac{\kappa_2 y}{x}+1\right)^2} \geq 0, \qquad (82)$$

so that

$$\mathbf{t}^T \bigtriangledown^2 \psi(x,y)\mathbf{t} \leq 0, \qquad (83)$$

when $\kappa_1 > \kappa_2 \geq 0$, $x \geq 0$, and $y \geq 0$. Therefore, the Hessian $\psi(x,y)$ is a negative semi-definite matric and $\psi(x,y)$ is a concave function w.r.t. x and y.

C. Proof of Lemma 3

If UAV m allocates a non-negative power for user k_U on subcarrier i in time slot n, i.e., $s_{m,k_U,i}[n] = 1$ and $\widetilde{p}_{m,k_U,i}[n] > 0$, under the condition $\mathcal{H}_{m,k_U,i}[n] \leq \mathcal{H}'_{m,k_E,i}[n]$, we have $\left[\tilde{R}_{m,k_U,i}[n] - \tilde{R}'_{m,k_U,k_E,i}[n]\right] \leq 0$, which leads to a smaller objective value in (21). Besides, the solution set becomes smaller as some power is wasted without improving the objective value. Hence, $\widetilde{p}_{m,k_U,i}[n] > 0$ for $\mathcal{H}_{m,k_U,i}[n] < \mathcal{H}'_{m,k_E,i}[n]$ is not an optimal solution.

REFERENCES

[1] R. Li, Z. Wei, L. Yang, D. W. Kwan Ng, N. Yang, J. Yuan, and J. An, "Joint trajectory and resource allocation design for UAV communication systems," in *2018 IEEE Globecom Workshops (GC Wkshps)*, Dec. 2018, pp. 1–6.

[2] J. An, K. Yang, J. Wu, N. Ye, S. Guo, and Z. Liao, "Achieving sustainable ultra-dense heterogeneous networks for 5G," *IEEE Commun. Mag.*, vol. 55, no. 12, pp. 84–90, Dec. 2017.

[3] K. Yang, N. Yang, N. Ye, M. Jia, Z. Gao, and R. Fan, "Non-orthogonal multiple access: Achieving sustainable future radio access," *IEEE Commun. Mag.*, vol. 57, no. 2, pp. 116–121, Feb. 2019.

[4] X. Gao, P. Wang, D. Niyato, K. Yang, and J. An, "Auction-based time scheduling for backscatter-aided RF-powered cognitive radio networks," *IEEE Trans. Wireless Commun.*, vol. 18, no. 3, pp. 1684–1697, Mar. 2019.

[5] V. W. Wong and L.-C. Wang, *Key Technologies for 5G Wireless Systems.* Cambridge University Press, 2017.

[6] Y. Zeng, R. Zhang, and T. J. Lim, "Wireless communications with unmanned aerial vehicles: opportunities and challenges," *IEEE Commun. Mag.*, vol. 54, no. 5, pp. 36–42, May 2016.

[7] ——, "Throughput maximization for UAV-enabled mobile relaying systems," *IEEE Trans. Commun.*, vol. 64, no. 12, pp. 4983–4996, Dec. 2016.

[8] L. Xiao, Y. Xu, D. Yang, and Y. Zeng, "Secrecy energy efficiency maximization for UAV-enabled mobile relaying," *IEEE Transactions on Green Communications and Networking*, pp. 1–1, Oct. 2019.

[9] M. Mozaffari, W. Saad, M. Bennis, and M. Debbah, "Unmanned aerial vehicle with underlaid device-to-device communications: Performance and tradeoffs," *IEEE Trans. Wireless Commun.*, vol. 15, no. 6, pp. 3949–3963, Jun. 2016.

[10] X. Sun, C. Shen, D. W. K. Ng, and Z. Zhong, "Robust trajectory and resource allocation design for secure UAV-aided communications," in *2019 IEEE Intern. Conf. on Commun. Workshops (ICC Workshops)*, May 2019, pp. 1–6.

[11] Y. Zeng, X. Xu, and R. Zhang, "Trajectory design for completion time minimization in UAV-enabled multicasting," *IEEE Trans. Wireless Commun.*, vol. 17, no. 4, pp. 2233–2246, Apr. 2018.

[12] X. Sun, D. W. K. Ng, Z. Ding, Y. Xu, and Z. Zhong, "Physical layer security in UAV systems: Challenges and opportunities," *IEEE Wireless Commun. Mag.*, vol. 26, no. 5, pp. 40–47, Oct. 2019.

[13] Q. Wu, W. Mei, and R. Zhang, "Safeguarding wireless network with UAVs: A physical layer security perspective," *arXiv preprint arXiv:1902.02472*, 2019.

[14] G. Zhang, Q. Wu, M. Cui, and R. Zhang, "Securing UAV communications via joint trajectory and power control," *IEEE Trans. Wireless Commun.*, vol. 18, no. 2, pp. 1376–1389, Feb. 2019.

[15] M. Cui, G. Zhang, Q. Wu, and D. W. K. Ng, "Robust trajectory and transmit power design for secure UAV communications," *IEEE Trans. Veh. Technol.*, vol. 67, no. 9, pp. 9042–9046, Sep. 2018.

[16] Y. Cai, Z. Wei, R. Li, D. W. Kwan Ng, and J. Yuan, "Energy-efficient resource allocation for secure UAV communication systems," in *2019 IEEE Wireless Commun. and Networking Conf. (WCNC)*, Apr. 2019, pp. 1–8.

[17] A. Li, Q. Wu, and R. Zhang, "UAV-enabled cooperative jamming for improving secrecy of ground wiretap channel," *IEEE Wireless Commun. Lett.*, vol. 8, no. 1, pp. 181–184, Feb. 2019.

[18] C. Zhong, J. Yao, and J. Xu, "Secure UAV communication with cooperative jamming and trajectory control," *IEEE Commun. Lett.*, vol. 23, no. 2, pp. 286–289, Feb. 2019.

[19] Y. Li, R. Zhang, J. Zhang, S. Gao, and L. Yang, "Cooperative jamming for secure UAV communications with partial eavesdropper information," *IEEE Access*, pp. 1–1, Jul. 2019.

[20] H. Lee, S. Eom, J. Park, and I. Lee, "UAV-aided secure communications with cooperative jamming," *IEEE Trans. Veh. Technol.*, vol. 67, no. 10, pp. 9385–9392, Oct. 2018.

[21] G. Zhang, Q. Wu, M. Cui, and R. Zhang, "Securing UAV communications via trajectory optimization," in *GLOBECOM 2017 - 2017 IEEE Global Communications Conference*, Dec. 2017, pp. 1–6.

[22] K. P. Valavanis and G. J. Vachtsevanos, *Handbook of Unmanned Aerial Vehicles*. Springer Publishing Company, Incorporated, 2014.

[23] P. Zhao, W. Chen, and W. Yu, "Guidance law for intercepting target with multiple no-fly zone constraints," *The Aeronautical Journal*, vol. 121, no. 1244, pp. 1479–1501, Aug. 2017.

[24] Y. Gao, H. Tang, B. Li, and X. Yuan, "Joint trajectory and power design for UAV-enabled secure communications with no-fly zone constraints," *IEEE Access*, vol. 7, pp. 44 459–44 470, Apr. 2019.

[25] D. Xu, Y. Sun, D. W. K. Ng, and R. Schober, "Multiuser MISO UAV communications in uncertain environments with no-fly zones: Robust trajectory and resource allocation design," *arXiv preprint arXiv:1905.10731v2*, 2019.

[26] Q. Wu and R. Zhang, "Common throughput maximization in UAV-enabled OFDMA systems with delay consideration," *IEEE Trans. Commun.*, vol. 66, no. 12, pp. 6614–6627, Dec. 2018.

[27] W. Yu and W. Chen, "Guidance law with circular no-fly zone constraint," *Nonlinear Dynamics*, Nov. 2014.

[28] G. Ducard, K. C. Kulling, and H. P. Geering, "Evaluation of reduction in the performance of a small UAV after an aileron failure for an adaptive guidance system," in *2007 American Control Conference*, Jul. 2007, pp. 1793–1798.

[29] Z. Liang and Z. Ren, "Tentacle-based guidance for entry flight with no-fly zone constraint," *Journal of Guidance, Control, and Dynamics*, vol. 41, no. 4, pp. 996–1005, Dec. 2018.

[30] A. Colpaert, E. Vinogradov, and S. Pollin, "Aerial coverage analysis of cellular systems at LTE and mmwave frequencies using 3D city models," *Sensors*, vol. 18, no. 12, p. 4311, Dec. 2018.

[31] A. Al-Hourani, S. Kandeepan, and S. Lardner, "Optimal LAP altitude for maximum coverage," *IEEE Wireless Commun. Lett.*, vol. 3, no. 6, pp. 569–572, Dec. 2014.

[32] Y. Zeng and R. Zhang, "Energy-efficient UAV communication with trajectory optimization," *IEEE Trans. Wireless Commun.*, vol. 16, no. 6, pp. 3747–3760, Jun. 2017.

[33] Y. Sun, D. Xu, D. W. K. Ng, L. Dai, and R. Schober, "Optimal 3D-trajectory design and resource allocation for solar-powered UAV communication systems," *IEEE Trans. Commun.*, vol. 67, no. 6, pp. 4281–4298, Jun. 2019.

[34] S. Eom, H. Lee, J. Park, and I. Lee, "UAV-aided wireless communication design with propulsion energy constraint," in *2018 IEEE Intern. Conf. on Commun. (ICC)*, May 2018, pp. 1–6.

[35] Z. Yang, C. Pan, M. Shikh-Bahaei, W. Xu, M. Chen, M. Elkashlan, and A. Nallanathan, "Joint altitude, beamwidth, location, and bandwidth optimization for UAV-enabled communications," *IEEE Commun. Lett.*, vol. 22, no. 8, pp. 1716–1719, Aug. 2018.

[36] J. Lim, S. Kim, and D. Shin, "Two-step doppler estimation based on intercarrier interference mitigation for OFDM radar," *IEEE Antennas and Wireless Propagation Letters*, vol. 14, pp. 1726–1729, Apr. 2015.

[37] J. Li, Y. Zhang, Y. Zhang, W. Xiong, Y. Huang, and Z. Wang, "Fast tracking doppler compensation for OFDM-based LEO satellite data transmission," in *2016 2nd IEEE Intern. Conf. on Comput. and Commun. (ICCC)*, Oct. 2016, pp. 1814–1817.

[38] H. Wang and Q. Zhang, "The doppler effect of aviation communication in OFDM system," *Acta Electronica Sinica*, vol. 31, no. 6, pp. 812 – 15, Jun. 2003.

[39] C. E. Leiserson, R. L. Rivest, T. H. Cormen, and C. Stein, *Introduction to algorithms.* MIT press Cambridge, MA, 2001, vol. 6.

[40] L. D. Nguyen, A. Kortun, and T. Q. Duong, "An introduction of real-time embedded optimisation programming for UAV systems under disaster communication." *EAI Endorsed Trans. Indust. Netw. & Intellig. Syst.*, vol. 5, no. 17, pp. 1–8, Dec. 2018.

[41] D. W. K. Ng, E. S. Lo, and R. Schober, "Energy-efficient resource allocation in OFDMA systems with large numbers of base station antennas," *IEEE Trans. Wireless Commun.*, vol. 11, no. 9, pp. 3292–3304, Jul. 2012.

[42] S. Boyd and L. Vandenberghe, *Convex optimization.* Cambridge University Press, 2004.

[43] Y. Sun, D. W. K. Ng, J. Zhu, and R. Schober, "Robust and secure resource allocation for full-duplex MISO multicarrier NOMA systems," *IEEE Trans. Commun.*, vol. 66, no. 9, pp. 4119–4137, Sep. 2018.

[44] P. K. Gopala, L. Lai, and H. E. Gamal, "On the secrecy capacity of fading channels," *IEEE Trans. Inf. Theory*, vol. 54, no. 10, pp. 4687–4698, Oct. 2008.

[45] D. W. K. Ng, E. S. Lo, and R. Schober, "Secure resource allocation and scheduling for OFDMA decode-and-forward relay networks," *IEEE Trans. Wireless Commun.*, vol. 10, no. 10, pp. 3528–3540, Oct. 2011.

[46] Z. Wei, D. W. K. Ng, J. Yuan, and H. M. Wang, "Optimal resource allocation for power-efficient MC-NOMA with imperfect channel state information," *IEEE Trans. Commun.*, vol. 65, no. 9, pp. 3944–3961, Sep. 2017.

[47] Y. Sun, D. W. K. Ng, Z. Ding, and R. Schober, "Optimal joint power and subcarrier allocation for full-duplex multicarrier non-orthogonal multiple access systems," *IEEE Trans. Commun.*, vol. 65, no. 3, pp. 1077–1091, Mar. 2017.

[48] Y. Huang, W. Mei, J. Xu, L. Qiu, and R. Zhang, "Cognitive UAV communication via joint maneuver and power control," *arXiv preprint arXiv:1901.02804*, 2019.